

Inference for a Large Directed Acyclic Graph with Unspecified Interventions

Chunlin Li

*School of Statistics,
University of Minnesota,
Minneapolis, MN 55455, USA*

LI000007@UMN.EDU

Xiaotong Shen

*School of Statistics,
University of Minnesota,
Minneapolis, MN 55455, USA*

XSHEN@UMN.EDU

Wei Pan

*Division of Biostatistics,
University of Minnesota,
Minneapolis, MN 55455, USA*

PANXX014@UMN.EDU

Abstract

Inference of directed relations given some unspecified interventions, that is, the target of each intervention is unknown, is challenging. In this article, we test hypothesized directed relations with unspecified interventions. First, we derive conditions to yield an identifiable model. Unlike classical inference, testing directed relations requires identifying ancestors and relevant interventions of hypothesis-specific primary variables. Towards this end, we propose a peeling algorithm based on nodewise regressions to establish a topological order of primary variables. Moreover, we prove that the peeling algorithm yields a consistent estimator in low order polynomial time. Second, we propose a likelihood ratio test integrated with a data perturbation scheme to account for the uncertainty of identifying ancestors and interventions. Also, we show that the distribution of a data perturbation test statistic converges to the target distribution. Numerical examples demonstrate the utility and effectiveness of the proposed methods, including an application to infer gene regulatory networks. The implementation of the proposed methods is available at <https://github.com/chunlinli/intdag>.

Keywords: High-dimensional inference, data perturbation, structure learning, identifiability, peeling algorithm

1. Introduction

Directed relations are essential to explaining pairwise dependencies among multiple interacting units. In gene network analysis, regulatory gene-to-gene relations are a focus of biological investigation (Sachs et al., 2005), while in a human brain network, scientists investigate causal influences among regions of interest to understand how the brain functions through the regional effects of neurons (Liu et al., 2017). In such a situation, inferring directed effects without other information is generally impossible because of the lack of identifiability in a Gaussian directed acyclic graph (DAG) model, and hence external interventions are introduced to treat a non-identifiable situation (Heinze-Deml et al., 2018). For

instance, the genetic variants such as single-nucleotide polymorphisms (SNPs) can be, and indeed are increasingly, treated as external interventions to infer inter-trait causal relations in a quantitative trait network (Brown and Knowles, 2020) and gene interactions in a gene regulatory network (Teumer, 2018; Molstad et al., 2021). In neuroimaging analysis, scientists use randomized experimental stimuli as interventions to identify causal relations in a functional brain network (Grosse-Wentrup et al., 2016; Bergmann and Hartwigsen, 2021). However, the interventions in these studies often have unknown targets and off-target effects (Jackson et al., 2003; Eaton and Murphy, 2007). Consequently, inferring directed relations while identifying useful interventions for inference is critical. This paper focuses on the simultaneous inference of directed relations subject to unspecified interventions, that is, without known targets.

In a DAG model, the research has been centered on the reconstruction of directed relations in observational and interventional studies (van de Geer and Bühlmann, 2013; Oates et al., 2016; Heinze-Deml et al., 2018; Zheng et al., 2018; Yuan et al., 2019). For inference, Bayesian methods (Friedman and Koller, 2003; Luo and Zhao, 2011; Viinikka et al., 2020) have been popular. Yet, statistical inference remains under-studied, especially for interventional models in high dimensions (Peters et al., 2016; Rothenhäusler et al., 2019). Recently, for observational data, Janková and van de Geer (2018) propose a debiased test of the strength of a single directed relation and Li et al. (2019) derives a constrained likelihood ratio test for multiple directed relations.

Despite progress, challenges remain. First, inferring directed relations requires identifying a certain DAG topological order (van de Geer and Bühlmann, 2013), while the identifiability in a Gaussian DAG with unspecified interventions remains under-explored. Second, the inferential results should agree with the acyclicity requirement for a DAG. As a result, degenerate and intractable situations can occur, making inference greatly different from the classical ones. Third, likelihood-based methods for learning the DAG topological order often use permutation search (van de Geer and Bühlmann, 2013) or continuous optimization subject to the acyclicity constraint (Zheng et al., 2018; Yuan et al., 2019), where a theoretical guarantee of the actual estimate (instead of the global optimum) has not been established for these approaches. Recently, an important line of work (Ghoshal and Honorio, 2018; Rajendran et al., 2021; Rolland et al., 2022) has focused on order-based algorithms with computational and statistical guarantees. However, in Gaussian DAGs, existing methods often rely on some error scale assumptions (Peters and Bühlmann, 2014), which is sensitive to variable scaling like the common practice of standardizing variables. This drawback could limit their applications, especially in causal inference, as causal relations are typically invariant to scaling.

To address the above issues, we develop structure learning and inference methods for a Gaussian DAG with unspecified additive interventions. Unlike the existing approach where structure discovery and subsequent inference are treated separately, our proposal integrates DAG structure learning and testing directed relations (also known as the natural direct effect in causal inference), accounting for the uncertainty of structure learning for inference. With suitable interventions called instrumental variables (IVs), the proposed approach removes the restrictive error scale assumptions and delivers creditable outcomes with theoretical guarantees in low order polynomial time. This result indicates IVs, a well-known tool in causal inference, can play important roles in structure learning even if some interventions

do not meet the IV criterion. More specifically, our contributions are summarized as the following aspects.

- For modeling, we establish the identifiability conditions for a Gaussian DAG with unspecified interventions. In particular, the conditions allow interventions on more than one target, which is suitable for multivariate causal analysis (Murray, 2006). Moreover, we introduce the concepts of nondegeneracy and regularity for hypothesis testing under a DAG model to characterize the behavior of a test.
- For methodology, we develop likelihood ratio tests for directed edges and pathways in a super-graph of the true DAG, where the super-graph is formed by ancestral relations and candidate interventional relations, offering the topological order for inference. Furthermore, we reconstruct the super-graph by the peeling algorithm, which automatically meets the acyclicity requirement. By integrating structure learning with inference, we account for the uncertainty of the super-graph estimation for the proposed tests via a novel data perturbation (DP) scheme, which effectively controls the type-I error while enjoying high statistical power.
- For theory, we prove that the proposed peeling algorithm based on nodewise regressions yields consistent results in $O(p \times \log \kappa_{\max}^{\circ} \times (q^3 + nq^2))$ operations almost surely, where p, q are the numbers of primary and intervention variables, n is the sample size, and κ_{\max}° is the sparsity. On this basis, we justify the proposed DP inference method by establishing the convergence of the DP likelihood ratio to the null distribution and desired power properties.
- The numerical studies and real data analysis demonstrate the utility and effectiveness of the proposed methods. The implementation of the proposed tests and structure learning method is available at <https://github.com/chunlinli/intdag>.

The rest of the article is structured as follows. Section 2 establishes model identifiability and introduces the concepts of nondegeneracy and regularity. Section 3 develops the proposed methods for structure learning and statistical inference. Section 4 presents statistical theory to justify the proposed methods. Section 5 performs simulation studies, followed by an application to infer gene pathways with gene expression and SNP data in Section 6. Section 7 concludes the article. The Appendix contains illustrative examples and technical proofs.

2. Gaussian directed acyclic graph with additive interventions

To infer directed relations among primary variables (variables of primary interest) $\mathbf{Y} = (Y_1, \dots, Y_p)^\top$, consider a structural equation model with additive interventions:

$$\mathbf{Y} = \mathbf{U}^\top \mathbf{Y} + \mathbf{W}^\top \mathbf{X} + \boldsymbol{\varepsilon}, \quad \boldsymbol{\varepsilon} \sim N(\mathbf{0}, \boldsymbol{\Sigma}), \quad \boldsymbol{\Sigma} = \text{Diag}(\sigma_1^2, \dots, \sigma_p^2), \quad (1)$$

where $\mathbf{X} = (X_1, \dots, X_q)^\top$ is a vector of additive intervention variables, $\mathbf{U} \in \mathbb{R}^{p \times p}$ and $\mathbf{W} \in \mathbb{R}^{q \times p}$ are unknown coefficient matrices, and $\boldsymbol{\varepsilon} = (\varepsilon_1, \dots, \varepsilon_p)^\top$ is a vector of random errors with $\sigma_j^2 > 0; j = 1, \dots, p$. In (1), $\boldsymbol{\varepsilon}$ is independent of \mathbf{X} but components of \mathbf{X} can be

dependent. The matrix \mathbf{U} specifies the directed relations among \mathbf{Y} , where $U_{kj} \neq 0$ if Y_k is a direct cause of Y_j , denoted by $Y_k \rightarrow Y_j$, and Y_k is called a parent of Y_j or Y_j a child of Y_k . Thus, \mathbf{U} represents a directed graph, which is required to be acyclic to ensure the validity of the local Markov property (Spirtes et al., 2000). The matrix \mathbf{W} specifies the targets and strengths of interventions, where $W_{lj} \neq 0$ indicates X_l intervenes on Y_j , denoted by $X_l \rightarrow Y_j$. In (1), no directed edge from a primary variable Y_j to an intervention variable X_l is permissible.

In what follows, we will focus on the DAG G with nodes $\mathbf{Y} = (Y_1, \dots, Y_p)$, primary variable edges $\mathcal{E} = \{(k, j) : U_{kj} \neq 0\}$, and intervention edges $\mathcal{I} = \{(l, j) : W_{lj} \neq 0\}$.

2.1 Identifiability

Model (1) is generally non-identifiable without interventions ($\mathbf{W} = \mathbf{0}$) when errors do not meet some requirements such as the equal-variance assumption (Peters and Bühlmann, 2014) and its variants (Ghoshal and Honorio, 2018; Rajendran et al., 2021). Moreover, a model can be identified when ε in (1) is replaced by non-Gaussian errors (Shimizu et al., 2006) or linear relations are replaced by nonlinear ones (Hoyer et al., 2009). Regardless, suitable interventions can make (1) identifiable. When intervention targets are known, the identifiability issue has been studied (Oates et al., 2016; Chen et al., 2018). However, it is less so when the exact targets and strengths of interventions are unknown, as in many biological applications (Jackson et al., 2003; Kulkarni et al., 2006), referring to the case of *unspecified* or *uncertain* interventions (Heinze-Deml et al., 2018; Eaton and Murphy, 2007; Squires et al., 2020).

We now categorize interventions as instruments and invalid instruments.

Definition 1 (Instrument) *An intervention is an instrument in a DAG if it satisfies:*

- (A) *(Relevance) it intervenes on at least one primary variable;*
- (B) *(Exclusion) it does not intervene on more than one primary variable.*

Otherwise, it is an invalid instrument.

Here, (A) requires an intervention to be active, while (B) prevents simultaneous interventions of a single intervention variable on multiple primary variables. This is critical to identifiability because in this situation an instrument on a cause variable Y_1 helps reveal its directed effect on an outcome variable Y_2 , which would otherwise be impossible. Thus, the instruments are introduced to break the symmetry that results in non-identifiability of directed relations $Y_1 \rightarrow Y_2$ and $Y_2 \rightarrow Y_1$.

Next, we make some assumptions on intervention variables to yield an identifiable model, where dependencies among intervention variables are permissible.

Assumption 1 *Assume that model (1) satisfies the following conditions.*

- (1A) *(Positive definiteness) $\mathbb{E} \mathbf{X} \mathbf{X}^\top$ is positive definite, where \mathbb{E} is the expectation.*
- (1B) *(Local faithfulness) $\text{Cov}(Y_j, X_l \mid \mathbf{X}_{\{1, \dots, q\} \setminus \{l\}}) \neq 0$ when X_l intervenes on Y_j , where Cov denotes the covariance.*

(1C) (*Instrumental sufficiency*) Each primary variable is intervened by at least one instrument.

Assumption 1A imposes mild distributional restrictions on \mathbf{X} , permitting discrete variables such as SNPs. Assumption 1B requires interventional effects not to cancel out as multiple targets from an invalid instrument are permitted. Importantly, if either Assumption 1B or Assumption 1C fails, model (1) is generally not identifiable, as shown in Example 2 of Appendix A.1. In Section 5, we empirically examine the situation when Assumption 1C is not met.

Proposition 1 (Identifiability) *Under Assumption 1, the parameters $(\mathbf{U}, \mathbf{W}, \boldsymbol{\Sigma})$ in model (1) are identifiable.*

Proposition 1 (proved in Appendix B.1) is derived for a DAG model with unspecified interventions. This is in contrast to Proposition 1 of Chen et al. (2018), which proves the identifiability of the parameters in a directed graph with target-known instruments on each primary variable. Moreover, it is worth noting that the estimated graph in Chen et al. (2018) may be cyclic and lacks the local Markov property for causal interpretation (Spirtes et al., 2000).

2.2 Likelihood-based inference for a DAG

Our primary goal is to perform statistical inference of directed edges and pathways. Let $\mathcal{H} \subseteq \{(k, j) : k \neq j, 1 \leq k, j \leq p\}$ be an edge set among primary variables $\{Y_1, \dots, Y_p\}$, where $(k, j) \in \mathcal{H}$ specifies a (hypothesized) directed edge $Y_k \rightarrow Y_j$ in (1). We shall focus on two types of testing with null and alternative hypotheses H_0 and H_a . For simultaneous testing of directed edges,

$$H_0 : U_{kj} = 0; \text{ for all } (k, j) \in \mathcal{H} \quad \text{versus} \quad H_a : U_{kj} \neq 0 \text{ for some } (k, j) \in \mathcal{H}; \quad (2)$$

for simultaneous testing of pathways,

$$H_0 : U_{kj} = 0; \text{ for some } (k, j) \in \mathcal{H} \quad \text{versus} \quad H_a : U_{kj} \neq 0 \text{ for all } (k, j) \in \mathcal{H}, \quad (3)$$

where $(\mathbf{U}_{\mathcal{H}^c}, \mathbf{W}, \boldsymbol{\Sigma})$ are unspecified nuisance parameters and c is the set complement.

Note that H_0 in (3) is a composite hypothesis that can be decomposed into sub-hypotheses

$$H_{0,\nu} : U_{k_\nu, j_\nu} = 0, \quad \text{versus} \quad H_{a,\nu} : U_{k_\nu, j_\nu} \neq 0; \quad \nu = 1, \dots, |\mathcal{H}|,$$

where $\mathcal{H} = \{(k_1, j_1), \dots, (k_{|\mathcal{H}|}, j_{|\mathcal{H}|})\}$ and each sub-hypothesis is a directed edge test.

Now consider likelihood inference for (2). Given an independent and identically distributed sample $(\mathbf{Y}_i, \mathbf{X}_i)_{i=1}^n$ from (1), the log-likelihood is

$$L(\boldsymbol{\theta}, \boldsymbol{\Sigma}) = -\frac{1}{2} \sum_{i=1}^n \|\boldsymbol{\Sigma}^{-1/2}((\mathbf{I} - \mathbf{U}^\top) \mathbf{Y}_i - \mathbf{W}^\top \mathbf{X}_i)\|_2^2 - n \log \sqrt{\det(\boldsymbol{\Sigma})}, \quad (4)$$

where $\boldsymbol{\theta} = (\mathbf{U}, \mathbf{W})$, $\boldsymbol{\Sigma} = \text{Diag}(\sigma_1^2, \dots, \sigma_p^2)$, and \mathbf{U} is subject to the acyclicity constraint (Zheng et al., 2018; Yuan et al., 2019) that no directed cycle is permissible in a DAG.

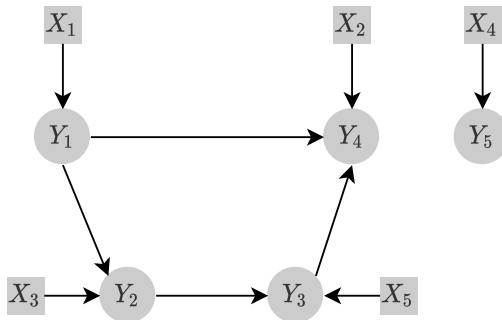


Figure 1: A true DAG structure of five primary variables Y_1, \dots, Y_5 and five intervention variables X_1, \dots, X_5 , where directed edges are represented by solid arrows while dependencies among \mathbf{X} are not displayed.

The likelihood ratio is defined as $Lr = L(\hat{\boldsymbol{\theta}}^{(1)}, \hat{\boldsymbol{\Sigma}}) - L(\hat{\boldsymbol{\theta}}^{(0)}, \hat{\boldsymbol{\Sigma}})$, where $\hat{\boldsymbol{\theta}}^{(1)}$ is a maximum likelihood estimate (MLE) in (4) subject to the acyclicity constraint, $\hat{\boldsymbol{\theta}}^{(0)}$ is an MLE subject to an additional requirement $\mathbf{U}_{\mathcal{H}} = \mathbf{0}$, and $\hat{\boldsymbol{\Sigma}}$ is an estimator of $\boldsymbol{\Sigma}$.

In many statistical models, a likelihood ratio has a nondegenerate and tractable distribution, for instance, a chi-squared distribution with degrees of freedom $|\mathcal{H}|$. However, in (1), because of the acyclicity constraint, some hypothesized edges in \mathcal{H} can be absent given the edge subset $\mathcal{E} \cap \mathcal{H}^c$ defined by the nonzero elements of nuisance parameter $\mathbf{U}_{\mathcal{H}^c}$, where \mathcal{E} denotes the edge set of the whole DAG. As a result, Lr may converge to a distribution with degrees of freedom less than $|\mathcal{H}|$ and the distribution may be even intractable, making inference for a DAG greatly different from the classical ones, as illustrated by Example 1.

Example 1 Consider the likelihood ratio test under null H_0 and alternative H_a for the DAG displayed in Figure 1. Let \mathcal{E} be the edge set of the DAG.

- $H_0 : U_{21} = 0$ versus $H_a : U_{21} \neq 0$, where $\mathcal{H} = \{(2, 1)\}$. Here, $(2, 1)$ forms a cycle together with the edges in $\mathcal{E} \cap \mathcal{H}^c$ (namely the edges not considered by the hypothesis), violating the acyclicity constraint. Note that the maximum likelihood value $L(\hat{\boldsymbol{\theta}}, \hat{\boldsymbol{\Sigma}})$ with $U_{21} \neq 0$ tends to be smaller than that with $U_{21} = 0$ when a random sample is obtained under H_0 , especially so when the asymptotics kicks in as the sample size increases. Consequently, the likelihood ratio Lr becomes zero, constituting a degenerate situation.
- $H_0 : U_{45} = U_{53} = 0$ versus $H_a : U_{45} \neq 0$ or $U_{53} \neq 0$, where $\mathcal{H} = \{(4, 5), (5, 3)\}$. In this case, $\{(4, 5), (5, 3)\}$ forms a cycle with the edges in $\mathcal{E} \cap \mathcal{H}^c$, violating the acyclicity constraint. Since the likelihood value $L(\boldsymbol{\theta}, \boldsymbol{\Sigma})$ tends to be maximized under the true graph when data is sampled under H_0 , we have $L(\hat{\boldsymbol{\theta}}^{(1)}, \hat{\boldsymbol{\Sigma}}) = \max(L(\hat{U}_{45}, \hat{U}_{53} = 0, \hat{\mathbf{U}}_{\mathcal{H}^c}, \hat{\mathbf{W}}, \hat{\boldsymbol{\Sigma}}), L(\hat{U}_{45} = 0, \hat{U}_{53}, \hat{\mathbf{U}}_{\mathcal{H}^c}, \hat{\mathbf{W}}, \hat{\boldsymbol{\Sigma}}))$. As a result, the likelihood ratio distribution becomes complicated in this situation due to the dependence between the two components in $L(\hat{\boldsymbol{\theta}}^{(1)}, \hat{\boldsymbol{\Sigma}})$.

Motivated by Example 1, we introduce the concepts of nondegeneracy and regularity.

Definition 2 (Nondegeneracy and regularity with respect to DAG)

- (A) An edge $(k, j) \in \mathcal{H}$ is nondegenerate with respect to DAG G if $\{(k, j)\} \cup \mathcal{E}$ contains no directed cycle, where \mathcal{E} denotes the edge set of G . Otherwise, (k, j) is degenerate. Let $\mathcal{D} \subseteq \mathcal{H}$ be the set of all nondegenerate edges with respect to G . A null hypothesis H_0 is nondegenerate with respect to DAG G if $\mathcal{D} \neq \emptyset$. Otherwise, H_0 is degenerate.
- (B) A null hypothesis H_0 is said to be regular with respect to DAG G if $\mathcal{D} \cup \mathcal{E}$ contains no directed cycle, where \mathcal{E} denotes the edge set of G . Otherwise, H_0 is called irregular.

Remark 1 In practice, \mathcal{D} is unknown and needs to be estimated from data.

Nondegeneracy ensures nonnegativity of the likelihood ratio. In testing (2), regularity excludes intractable situations for the null distribution. In testing (3), if H_0 is irregular, then $\mathcal{D} \cup \mathcal{E}$ has a directed cycle, which means the hypothesized directed pathway cannot exist due to the acyclicity constraint. Thus, regularity excludes the degenerate situations in testing (3).

In what follows, we mainly focus on nondegenerate and regular hypotheses. For the degenerate case, the p-value is defined to be one. For the irregular case of edge test (2), we decompose the hypothesis into regular sub-hypotheses and conduct multiple testing. For the irregular case of pathway test (3), the p-value is defined to be one. More discussions on the implementation in irregular cases are provided in Appendix A.5.

Finally, we introduce some notations for a DAG G with primary variables $\{Y_1, \dots, Y_p\}$, intervention variables $\{X_1, \dots, X_q\}$, a directed edge set $\mathcal{E} \subseteq \{(k, j) : k \neq j, 1 \leq k, j \leq p\}$, and an intervention edge set $\mathcal{I} \subseteq \{(l, j) : 1 \leq l \leq q, 1 \leq j \leq p\}$. If there is a directed path $Y_k \rightarrow \dots \rightarrow Y_j$ in G , Y_k is called an ancestor of Y_j or Y_j a descendant of Y_k . Let $\mathcal{A} = \{(k, j) : Y_k \rightarrow \dots \rightarrow Y_j\}$ be the set of all ancestral relations. In a DAG G , let $\text{PA}_G(j) = \{k : (k, j) \in \mathcal{E}\}$, $\text{AN}_G(j) = \{k : (k, j) \in \mathcal{A}\}$, $\text{D}_G(j) = \{k : (k, j) \in \mathcal{D}\}$, and $\text{IN}_G(j) = \{l : (l, j) \in \mathcal{I}\}$ be the parent, ancestor, nondegenerate hypothesized parent, and intervention sets of Y_j , respectively.

3. Methodology

This section develops the main methodology, including the peeling algorithm for structure learning and the data perturbation inference for simultaneous testing of directed edges (2) and pathways (3).

One major challenge to the likelihood approach is optimization subject to the acyclicity requirement. This constraint imposes difficulty on not only computation but also asymptotic theory. As a result, there is a gap between the asymptotic distribution based on a global maximum and that on the actual estimate which could be a local maximum (Janková and van de Geer, 2018; Li et al., 2019). Moreover, the actual estimate may give an imprecise topological order, tending to impact adversely on inference.

To circumvent the acyclicity requirement, we propose using a super-graph S of the true DAG G , where S is constructed by a novel peeling method without explicitly imposing the acyclicity constraint. As a result, our method is scalable with a statistical guarantee of the actual estimate. We will focus on a specific super-graph S consisting of primary variable

edges $\mathcal{E}_S := \mathcal{A} \supseteq \mathcal{E}$ and candidate intervention edges $\mathcal{I}_S := \mathcal{C} \supseteq \mathcal{I}$, where \mathcal{E} and \mathcal{I} are sets of primary variable edges and intervention edges in the original graph G , and set \mathcal{C} is to be defined shortly after (6). Note that S , whose primary variable edges consist of all ancestral relations of G , is also a DAG. Given the super-graph S , the true DAG G can be reconstructed by nodewise constrained regressions.

Let $\boldsymbol{\theta}_S = (\mathbf{U}_{\mathcal{A}}, \mathbf{W}_{\mathcal{C}})$ be $\boldsymbol{\theta}$ restricted to S . Note that $\boldsymbol{\theta}_{S^c} = (\mathbf{U}_{\mathcal{A}^c}, \mathbf{W}_{\mathcal{C}^c}) = \mathbf{0}$ in the original graph G . Given S , the log-likelihood $L(\boldsymbol{\theta}, \boldsymbol{\Sigma})$ in (4) can be rewritten as

$$L_S(\boldsymbol{\theta}_S, \boldsymbol{\Sigma}) = - \sum_{j=1}^p \left(\text{RSS}_j(\boldsymbol{\theta}_S) / 2\sigma_j^2 + \log \sqrt{2\pi\sigma_j^2} \right), \quad (5)$$

$$\text{RSS}_j(\boldsymbol{\theta}_S) = \sum_{i=1}^n \left(Y_{ij} - \sum_{(k,j) \in \mathcal{A}} U_{kj} Y_{ik} - \sum_{(l,j) \in \mathcal{C}} W_{lj} X_{il} \right)^2,$$

which involves $|\mathcal{A}| + |\mathcal{C}|$ parameters for $\boldsymbol{\theta}_S$.

Our plan is as follows. In Section 3.1, we hierarchically construct S via nodewise regressions of Y_j over \mathbf{X} ; $j = 1, \dots, p$ without the acyclicity constraint for \mathbf{U} . Then in Section 3.2, on the ground of constructed super-graph S and (5), we develop likelihood ratio tests for hypotheses (2) and (3).

3.1 Structure learning via peeling

This section develops a novel structure learning method based on a peeling algorithm and nodewise constrained regressions to construct $S = (\mathcal{A}, \mathcal{C})$ in a hierarchical manner.

First, we observe an important connection between primary variables and intervention variables. Rewrite (1) as

$$\mathbf{Y} = \mathbf{V}^\top \mathbf{X} + \boldsymbol{\varepsilon}_V, \quad \boldsymbol{\varepsilon}_V = (\mathbf{I} - \mathbf{U}^\top)^{-1} \boldsymbol{\varepsilon} \sim N(\mathbf{0}, \boldsymbol{\Omega}^{-1}), \quad (6)$$

where $\boldsymbol{\Omega} = (\mathbf{I} - \mathbf{U})\boldsymbol{\Sigma}^{-1}(\mathbf{I} - \mathbf{U}^\top)$ is a precision matrix and $\mathbf{V} = \mathbf{W}(\mathbf{I} - \mathbf{U})^{-1}$. Now, define the set of candidate interventional relations $\mathcal{C} := \{(l, j) : V_{lj} \neq 0\}$.

Proposition 2 *Suppose Assumption 1 is satisfied. Then $\mathcal{C} \supseteq \mathcal{I}$. Moreover,*

- (A) *if $V_{lj} \neq 0$, then X_l intervenes on Y_j or an ancestor of Y_j ;*
- (B) *Y_j is a leaf variable (having no child) if and only if there is an instrument X_l such that $V_{lj} \neq 0$ and $V_{lj'} = 0$ for $j' \neq j$.*

The proof of Proposition 2 is deferred to Appendix B.2. Intuitively, $V_{lj} \neq 0$ implies the dependence of Y_j on X_l through a directed path $X_l \rightarrow \dots \rightarrow Y_j$, and hence that X_l intervenes on Y_j or an ancestor of Y_j . Thus, the instruments on a leaf variable are independent of the other primary variables conditional on the rest of interventions. This observation suggests a method to reconstruct the DAG topological order by sequentially identifying the leaves in the DAG and removing the identified leaf variables.

Next, we discuss the estimation of \mathbf{V} and construction of S .

3.1.1 NODEWISE CONSTRAINED REGRESSIONS

We propose nodewise ℓ_0 -constrained regressions to estimate nonzero elements of \mathbf{V} :

$$\widehat{\mathbf{V}}_{\cdot j} = \arg \min_{\mathbf{V}_{\cdot j}} \sum_{i=1}^n (Y_{ij} - \mathbf{V}_{\cdot j}^\top \mathbf{X}_i)^2 \quad \text{s.t.} \quad \sum_{l=1}^q \mathbf{I}(V_{lj} \neq 0) \leq \kappa_j; \quad j = 1, \dots, p, \quad (7)$$

where $1 \leq \kappa_j \leq q$ is an integer-valued tuning parameter controlling the sparsity of $\mathbf{V}_{\cdot j}$ and can be chosen by BIC or cross-validation.

To solve (7), we use $J_{\tau_j}(z) = \min(|z|/\tau_j, 1)$ as a surrogate of the ℓ_0 -function $\mathbf{I}(z \neq 0)$ (Shen et al., 2012) and develop a difference-of-convex (DC) algorithm with the ℓ_0 -projection to improve globality of the solution of (7). At $(t+1)$ th iteration, we solve a weighted Lasso problem,

$$\widetilde{\mathbf{V}}_{\cdot j}^{[t+1]} = \arg \min_{\mathbf{V}_{\cdot j}} \sum_{i=1}^n (Y_{ij} - \mathbf{V}_{\cdot j}^\top \mathbf{X}_i)^2 + 2n\gamma_j\tau_j \sum_{l=1}^q \mathbf{I}(|\widetilde{V}_{lj}^{[t]}| \leq \tau_j) |V_{lj}|; \quad j = 1, \dots, p, \quad (8)$$

where $\gamma_j > 0$ is a tuning parameter and $\widetilde{\mathbf{V}}_{\cdot j}^{[t]}$ is the solution of (8) at the t -th iteration. The DC algorithm terminates at $\widetilde{\mathbf{V}}_{\cdot j} = \widetilde{\mathbf{V}}_{\cdot j}^{[t]}$ such that $\|\widetilde{\mathbf{V}}_{\cdot j}^{[t+1]} - \widetilde{\mathbf{V}}_{\cdot j}^{[t]}\|_\infty \leq \sqrt{\text{tol}}$, where tol is the machine precision. Then, we obtain the solution $\widehat{\mathbf{V}}_{\cdot j}$ of (7) by projecting $\widetilde{\mathbf{V}}_{\cdot j}$ onto the ℓ_0 -constrained set $\{\|\mathbf{V}_{\cdot j}\|_0 \leq \kappa_j\}$.

Algorithm 1: Constrained minimization via DC programming + ℓ_0 projection

- 1 Specify $\gamma_j > 0$, $\tau_j > 0$, and $1 \leq \kappa_j \leq q$. Initialize $\widetilde{\mathbf{V}}_{\cdot j}^{[0]}$ with $|\{l : \widetilde{V}_{lj}^{[0]} > \tau_j\}| \leq \kappa_j$.
- 2 Compute $\widetilde{\mathbf{V}}_{\cdot j} = \widetilde{\mathbf{V}}_{\cdot j}^{[t]}$ such that $\|\widetilde{\mathbf{V}}_{\cdot j}^{[t+1]} - \widetilde{\mathbf{V}}_{\cdot j}^{[t]}\|_\infty \leq \sqrt{\text{tol}}$.
- 3 (ℓ_0 -projection) Let $B_j = \{l : \sum_{l'=1}^q \mathbf{I}(|\widetilde{V}_{l'j}| \geq |\widetilde{V}_{lj}|) \leq \kappa_j\}$. Set

$$\widehat{\mathbf{V}}_{\cdot j} = \arg \min_{\mathbf{V}_{\cdot j}} \|\mathbf{Y}_j - \mathbf{V}_{\cdot j}^\top \mathbf{X}\|_2^2 \quad \text{s.t.} \quad V_{lj} = 0 \text{ for } l \notin B_j.$$

3.1.2 PEELING

Now, we describe a *peeling* algorithm to estimate $S = (\mathcal{A}, \mathcal{C})$ based on \mathbf{V} .

Before proceeding, we introduce the notion of *topological height* to characterize the DAG topological order. Given a DAG G , the height $h_G(j)$ of Y_j is defined as the maximal length of a directed path from Y_j to a leaf variable, where $0 \leq h_G(j) \leq p-1$ with a leaf having zero height. Then the primary variables of the same height form a topological layer and the layers constitute a partition of primary variables in G . For instance, in Figure 1, $\{Y_4, Y_5\}$, $\{Y_3\}$, $\{Y_2\}$, $\{Y_1\}$ are topological layers with height 0, 1, 2, 3, respectively.

Observe that the topological layer of height h are leaves in the sub-graph with primary variables of height no less than h . Based on Proposition 2, the peeling algorithm sequentially identifies and peels off the primary variables of height h ; $h = 0, 1, 2, \dots$. Note that instruments in the sub-graph may not be necessarily the instruments in the graph G after some primary variables are removed. However, the next proposition indicates that the instruments in the corresponding sub-graph remain useful to reconstruct ancestral relations.

Algorithm 2: Reconstruction of topological layers by peeling

- 1 Let $\widehat{\mathbf{V}}^{[0]} = \widehat{\mathbf{V}}$. Begin iteration with $h = 0, \dots$: at iteration h ,
- 2 In the current sub-graph identify all instrument-leaf pairs $X_l \rightarrow Y_j$ satisfying

$$l = \arg \min_{l': \|\widehat{\mathbf{V}}_{l'}^{[h]}\|_0 \neq 0} \|\widehat{\mathbf{V}}_{l'}^{[h]}\|_0 \text{ and } j = \arg \max_{j'} |\widehat{\mathbf{V}}_{l_j'}^{[h]}|. \text{ Let } h_{\widehat{G}}(j) = h.$$
- 3 For a leaf Y_k , identify all directed relations $Y_k \rightarrow Y_j$ with $h_{\widehat{G}}(j) = h - 1$ when $\widehat{\mathbf{V}}_{l_j} \neq 0$ for each instrument X_l of Y_k in the current sub-graph.
- 4 Peeling-off all the leaves Y_j by deleting j th columns from $\widehat{\mathbf{V}}^{[h]}$ to yield $\widehat{\mathbf{V}}^{[h+1]}$.
- 5 Repeat Steps 2-4 until all primary variables are removed.
- 6 Compute $\widehat{S} = (\widehat{\mathcal{A}}, \widehat{\mathcal{C}})$ and $\widehat{\mathcal{D}}$:

$$\begin{aligned} \widehat{\mathcal{A}} &= \{(k, j) : Y_k \rightarrow \dots \rightarrow Y_j\}, & \widehat{\mathcal{D}} &= \{(k, j) \in \mathcal{H} : (j, k) \notin \widehat{\mathcal{A}}\}, \\ \widehat{\mathcal{C}} &= \{(l, j) : |\widehat{\mathbf{V}}_{l_j}| > \tau_j\}, \text{ where } \tau_j \text{ is specified in Algorithm 1.} \end{aligned}$$

Proposition 3 *Let Y_k have height $h_G(k)$. Let G' be the sub-graph with primary variables of height $\geq h_G(k)$. Under Assumption 1, for a pair (k, j) with $h_G(j) = h_G(k) - 1$, we have $Y_k \rightarrow Y_j$ if and only if $V_{l_j} \neq 0$ for each instrument X_l of Y_k in G' .*

Proposition 3 (proved in Appendix B.3) permits the construction of directed relations between the topological layers of heights h and $h - 1$; $h \geq 1$ and thus ancestral relations.

The peeling algorithm is summarized in Algorithm 2 and a detailed illustration is presented in Example 3 of Appendix A.2.

Remark 2 (Recovery of true graph G) $\widehat{\mathcal{A}}$ estimates a superset of directed relations of \mathbf{U} and $\widehat{\mathcal{C}}$ a superset of interventional relations of \mathbf{W} . Therefore, under some technical conditions, with suitable tuning parameters, the true graph G can be reconstructed by estimating (\mathbf{U}, \mathbf{W}) through ℓ_0 -constrained regressions given the estimated super-graph $\widehat{S} = (\widehat{\mathcal{A}}, \widehat{\mathcal{C}})$,

$$\begin{aligned} \min_{(\mathbf{U}_{\text{AN}_{\widehat{S}}(j),j}, \mathbf{W}_{\text{IN}_{\widehat{S}}(j),j})} & \sum_{i=1}^n \left(Y_{ij} - \mathbf{U}_{\text{AN}_{\widehat{S}}(j),j}^\top \mathbf{Y}_{i,\text{AN}_{\widehat{S}}(j)} - \mathbf{W}_{\text{IN}_{\widehat{S}}(j),j}^\top \mathbf{X}_{i,\text{IN}_{\widehat{S}}(j)} \right)^2 \\ \text{s.t.} & \sum_{k \in \text{AN}_{\widehat{S}}(j)} \mathbf{I}(U_{kj} \neq 0) + \sum_{l \in \text{IN}_{\widehat{S}}(j)} \mathbf{I}(W_{lj} \neq 0) \leq \kappa'_j. \end{aligned} \quad (9)$$

The final estimates $\widehat{\mathbf{U}}_{\cdot j} = \left(\widehat{\mathbf{U}}_{\text{AN}_{\widehat{S}}(j),j}, \mathbf{0}_{\text{AN}_{\widehat{S}}(j)^c} \right)$ and $\widehat{\mathbf{W}}_{\cdot j} = \left(\widehat{\mathbf{W}}_{\text{IN}_{\widehat{S}}(j),j}, \mathbf{0}_{\text{IN}_{\widehat{S}}(j)^c} \right)$; $j = 1, \dots, p$.

3.2 Likelihood ratio test via data perturbation

This subsection proposes an inference method for testing (2) and (3). We first construct a likelihood ratio $\text{Lr}(S, \boldsymbol{\Sigma})$ in given $(S, \boldsymbol{\Sigma})$ and then plug-in an estimate $(\widehat{S}, \widehat{\boldsymbol{\Sigma}})$. Next we perform a test via data perturbation, accounting for the uncertainty of constructing S .

3.2.1 LIKELIHOOD RATIO GIVEN S

Consider the test in (2). From (5), the likelihood ratio given (S, Σ) is

$$\text{Lr}(S, \Sigma) = L_S(\hat{\theta}_S^{(1)}, \Sigma) - L_S(\hat{\theta}_S^{(0)}, \Sigma) = \sum_{j=1}^p \frac{\text{RSS}_j(\hat{\theta}_S^{(0)}) - \text{RSS}_j(\hat{\theta}_S^{(1)})}{2\sigma_j^2}$$

where $\hat{\theta}_S^{(1)}$ is the MLE given (S, Σ) , and $\hat{\theta}_S^{(0)}$ is the MLE given (S, Σ) subject to $\mathbf{U}_{\mathcal{H}} = 0$.

Now, recall that $\text{D}_G(j) = \{k : (k, j) \in \mathcal{D}\}$, where \mathcal{D} is the set of nondegenerate edges of H_0 with respect to G (Definition 2). Of note, $\text{D}_S(j) = \text{D}_G(j)$ since an edge is nondegenerate with respect to S if and only if it is nondegenerate with respect to G . To eliminate the nuisance parameters, observe that if $\text{D}_S(j) = \emptyset$, then $\text{RSS}_j(\hat{\theta}_S^{(0)}) - \text{RSS}_j(\hat{\theta}_S^{(1)}) = 0$, because no H_0 constraint is imposed for Y_j . Hence, $\text{Lr}(S, \Sigma)$ only summarizes the contributions from the primary variables with nondegenerate hypothesized edges,

$$\text{Lr}(S, \Sigma) = \sum_{j: \text{D}_S(j) \neq \emptyset} \frac{\text{RSS}_j(\hat{\theta}_S^{(0)}) - \text{RSS}_j(\hat{\theta}_S^{(1)})}{2\sigma_j^2}, \quad (10)$$

where the nuisance parameters for Y_j with $\text{D}_S(j) = \emptyset$ are eliminated.

The likelihood ratio test statistic becomes $\text{Lr} = \text{Lr}(\hat{S}, \hat{\Sigma})$. Here, \hat{S} is constructed by Algorithm 2 in Section 3.1 and $\hat{\Sigma} = \text{Diag}(\hat{\sigma}_1^2, \dots, \hat{\sigma}_p^2)$,

$$\hat{\sigma}_j^2 = \frac{\text{RSS}_j(\hat{\theta}_{\hat{S}}^{(1)})}{n - |\text{AN}_{\hat{S}}(j)| - |\text{IN}_{\hat{S}}(j)|}, \quad j = 1, \dots, p, \quad (11)$$

where $\text{AN}_{\hat{S}}(j)$ and $\text{IN}_{\hat{S}}(j)$ are the estimated ancestor and candidate intervention sets of Y_j .

3.2.2 TESTING DIRECTED EDGES (2) VIA DATA PERTURBATION

The likelihood ratio requires an estimation of S , where we must account for the uncertainty of \hat{S} for accurate finite-sample inference.

To proceed, we consider the test statistic Lr based on a “correct” super-graph $S \supseteq S^\circ$, where $S = (\mathcal{A}, \mathcal{C}) \supseteq S^\circ = (\mathcal{A}^\circ, \mathcal{C}^\circ)$ means that $\mathcal{A} \supseteq \mathcal{A}^\circ$ and $\mathcal{C} \supseteq \mathcal{C}^\circ$ and $^\circ$ denotes the truth. Intuitively, a “correct” super-graph distinguishes descendants and nondescendants and thus can help to infer the true directed relations defined by the local Markov property (Spirtes et al., 2000) without introducing model errors, yet may lead to a less powerful test when S is much larger than S° . By comparison, a “wrong” graph $S \not\supseteq S^\circ$ provides an incorrect topological order, and a test based on a “wrong” graph may be biased, accompanied by an inflated type-I error.

Now, let $\mathbf{Z}_{n \times (p+q)} = (\mathbf{X}, \mathbf{Y})$ be the data matrix, where $\mathbf{Y}_{n \times p} = (\mathbf{Y}_1, \dots, \mathbf{Y}_n)^\top$ and $\mathbf{X}_{n \times q} = (\mathbf{X}_1, \dots, \mathbf{X}_n)^\top$. Moreover, let $\mathbf{e}_j \in \mathbb{R}^n$ be the j th column of error matrix $\mathbf{e}_{n \times p} = (\boldsymbol{\varepsilon}_1, \dots, \boldsymbol{\varepsilon}_n)^\top$. From (10), assuming $\hat{S} \supseteq S^\circ$ is a “correct” super-graph, the likelihood ratio

becomes

$$\begin{aligned}
 \text{Lr} &= \sum_{j:\text{D}_{\widehat{S}}(j) \neq \emptyset} \frac{\mathbf{Y}_j^\top (\mathbf{P}_{\widehat{A}_j} - \mathbf{P}_{\widehat{B}_j}) \mathbf{Y}_j}{2\widehat{\sigma}_j} \\
 &= \sum_{j:\text{D}_{\widehat{S}}(j) \neq \emptyset} \frac{(\mathbf{Y}_{\text{D}_{\widehat{S}}(j)} \mathbf{U}_{\text{D}_{\widehat{S}}(j),j} + \mathbf{e}_j)^\top (\mathbf{P}_{\widehat{A}_j} - \mathbf{P}_{\widehat{B}_j}) (\mathbf{Y}_{\text{D}_{\widehat{S}}(j)} \mathbf{U}_{\text{D}_{\widehat{S}}(j),j} + \mathbf{e}_j)}{2\widehat{\sigma}_j}, \quad (12) \\
 \widehat{\sigma}_j &= \frac{\mathbf{Y}_j^\top (\mathbf{I} - \mathbf{P}_{\widehat{A}_j}) \mathbf{Y}_j}{n - |\widehat{A}_j|} = \frac{\mathbf{e}_j^\top (\mathbf{I} - \mathbf{P}_{\widehat{A}_j}) \mathbf{e}_j}{n - |\widehat{A}_j|}; \quad 1 \leq j \leq p,
 \end{aligned}$$

where $\mathbf{P}_A = \mathbf{Z}_A (\mathbf{Z}_A^\top \mathbf{Z}_A)^{-1} \mathbf{Z}_A^\top$ is the projection matrix onto the span of columns A in \mathbf{Z} , $\widehat{A}_j = \text{AN}_{\widehat{S}}(j) \cup \text{IN}_{\widehat{S}}(j) \cup \text{D}_{\widehat{S}}(j)$, and $\widehat{B}_j = (\text{AN}_{\widehat{S}}(j) \cup \text{IN}_{\widehat{S}}(j)) \setminus \text{D}_{\widehat{S}}(j)$. Of note, $\mathbf{Y}_{\text{D}_{S}(j)} \mathbf{U}_{\text{D}_{S}(j),j} = \mathbf{0}$ for all j under H_0 , while $\mathbf{Y}_{\text{D}_{S}(j)} \mathbf{U}_{\text{D}_{S}(j),j} \neq \mathbf{0}$ for some j under H_a .

We propose a data perturbation (DP) method (Shen and Ye, 2002; Breiman, 1992) to approximate the null distribution of Lr in (12). The idea behind DP is to assess the sensitivity of the estimates through perturbed data $\mathbf{Y}_i^* = \mathbf{Y}_i + \boldsymbol{\varepsilon}_i^*$, where $\boldsymbol{\varepsilon}_i^* \sim N(0, \widehat{\boldsymbol{\Sigma}})$; $i = 1, \dots, n$.

Let $(\mathbf{Z}^*, \mathbf{e}^*) = (\mathbf{X}, \mathbf{Y}^*, \mathbf{e}^*)$ be perturbed data, where $\mathbf{e}_{n \times p}^* = (\mathbf{e}_1^*, \dots, \mathbf{e}_p^*) = (\boldsymbol{\varepsilon}_1^*, \dots, \boldsymbol{\varepsilon}_n^*)^\top$ denotes perturbation errors. Given $(\mathbf{Z}^*, \mathbf{e}^*)$, we obtain a perturbation estimate \widehat{S}^* . In (12), under H_0 , $\text{Lr} = f(\mathbf{X}, \boldsymbol{\mu}, \mathbf{e})$ is a function of intervention data \mathbf{X} , conditional mean $\boldsymbol{\mu} = \mathbb{E}(\mathbf{Y} | \mathbf{X}) \in \mathbb{R}^{n \times p}$ and unobserved error \mathbf{e} . However, the perturbation error \mathbf{e}^* is *known* given the DP sample $(\mathbf{Z}^*, \mathbf{e}^*)$, suggesting a form Lr^* based on Lr:

$$\text{Lr}^* \equiv f(\mathbf{X}, \mathbf{Y}, \mathbf{e}^*) = \sum_{j:\text{D}_{\widehat{S}}(j) \neq \emptyset} \frac{(\mathbf{e}_j^*)^\top (\mathbf{P}_{\widehat{A}_j^*} - \mathbf{P}_{\widehat{B}_j^*}) \mathbf{e}_j^*}{2\widetilde{\sigma}_j^*}, \quad \widetilde{\sigma}_j^* = \frac{(\mathbf{e}_j^*)^\top (\mathbf{I} - \mathbf{P}_{\widehat{A}_j^*}) \mathbf{e}_j^*}{n - |\widehat{A}_j^*|}, \quad 1 \leq j \leq p, \quad (13)$$

which mimics (12) when $\mathbf{Y}_{\text{D}_{S}(j)} \mathbf{U}_{\text{D}_{S}(j)} = \mathbf{0}$ under H_0 , with \mathbf{e}_j replaced by \mathbf{e}_j^* . As a result, when $\widehat{S}^* \supseteq S^\circ$, the conditional distribution of Lr^* given \mathbf{Z} well approximates the null distribution of Lr, where the model selection effect is accounted for by assessing the variability of \widehat{A}_j^* and \widehat{B}_j^* over different realizations of $(\mathbf{Z}^*, \mathbf{e}^*)$.

In practice, we use Monte-Carlo to approximate the distribution of Lr^* given \mathbf{Z} in (13). In particular, we generate M perturbed samples $(\mathbf{Z}_m^*, \mathbf{e}_m^*)_{m=1}^M$ independently and compute Lr_m^* ; $m = 1, \dots, M$. Then, we examine the condition $\widehat{S}_m^* \supseteq S^\circ$ by checking its empirical counterpart $\widehat{S}_m^* \supseteq \widehat{S}$. The DP p-value of edge test in (2) is defined as

$$\text{Pval} = \left(\sum_{m=1}^M \mathbb{I}(\text{Lr}_m^* \geq \text{Lr}, \widehat{S}_m^* \supseteq \widehat{S}) \right) / \left(\sum_{m=1}^M \mathbb{I}(\widehat{S}_m^* \supseteq \widehat{S}) \right), \quad (14)$$

where $\mathbb{I}(\cdot)$ is the indicator function.

Remark 3 Assume $\widehat{S}^* \supseteq S^\circ$ is a “correct” super-graph. A naive likelihood ratio based on perturbed data $(\mathbf{Z}^*, \mathbf{e}^*)$ is

$$\text{Lr}(\widehat{S}^*, \widehat{\boldsymbol{\Sigma}}^*) = \sum_{j:\text{D}_{\widehat{S}^*}(j) \neq \emptyset} \frac{(\mathbf{Y}_{\text{D}_{\widehat{S}^*}(j)} \mathbf{U}_{\text{D}_{\widehat{S}^*}(j),j} + \mathbf{e}_j + \mathbf{e}_j^*)^\top (\mathbf{P}_{\widehat{A}_j^*} - \mathbf{P}_{\widehat{B}_j^*}) (\mathbf{Y}_{\text{D}_{\widehat{S}^*}(j)} \mathbf{U}_{\text{D}_{\widehat{S}^*}(j),j} + \mathbf{e}_j + \mathbf{e}_j^*)}{2\widehat{\sigma}_j^*}.$$

Note that the error \mathbf{e}_j given \mathbf{Z} is deterministic and does not vanish under either H_0 or H_a ; $j = 1, \dots, p$. Thus, the conditional distribution of $Lr(\widehat{\mathbf{S}}^*, \widehat{\boldsymbol{\Sigma}}^*)$ given \mathbf{Z} does not approximate the null distribution of Lr in (12), in contrast to the DP likelihood ratio Lr^* in (13).

3.2.3 EXTENSION TO HYPOTHESIS TESTING FOR A PATHWAY

Next, we extend the DP inference for (3). Denote $\mathcal{H} = \{(k_1, j_1), \dots, (k_{|\mathcal{H}|}, j_{|\mathcal{H}|})\}$. Then the test of pathways in (3) can be reduced to testing sub-hypotheses

$$H_{0,\nu} : U_{k_\nu, j_\nu} = 0, \quad \text{versus} \quad H_{a,\nu} : U_{k_\nu, j_\nu} \neq 0; \quad \nu = 1, \dots, |\mathcal{H}|,$$

where each sub-hypothesis is a directed edge test. Given $(S, \boldsymbol{\Sigma})$, the likelihood ratio for $H_{0,\nu}$ is $Lr_\nu(S, \boldsymbol{\Sigma}) = L_S(\widehat{\boldsymbol{\theta}}_S^{(1)}, \boldsymbol{\Sigma}) - L_S(\widehat{\boldsymbol{\theta}}_S^{(0,\nu)}, \boldsymbol{\Sigma})$, where $\widehat{\boldsymbol{\theta}}_S^{(0,\nu)}$ is the MLE under the constraint that $U_{k_\nu, j_\nu} = 0$. Then for $\widehat{S} \supseteq S^\circ$, we have

$$\begin{aligned} Lr_\nu &= \frac{1}{2} \frac{(\mathbf{Y}_{k_\nu} U_{k_\nu, j_\nu} + \mathbf{e}_{j_\nu})^\top (\mathbf{P}_{\widehat{A}_{j_\nu}} - \mathbf{P}_{\widehat{B}_{j_\nu}}) (\mathbf{Y}_{k_\nu} U_{k_\nu, j_\nu} + \mathbf{e}_{j_\nu})}{(\mathbf{e}_{j_\nu})^\top (\mathbf{I} - \mathbf{P}_{\widehat{A}_{j_\nu}}) \mathbf{e}_{j_\nu} / (n - |\widehat{A}_{j_\nu}|)}, \\ Lr_\nu^* &= \frac{1}{2} \frac{(\mathbf{e}_{j_\nu}^*)^\top (\mathbf{P}_{\widehat{A}_{j_\nu}^*} - \mathbf{P}_{\widehat{B}_{j_\nu}^*}) \mathbf{e}_{j_\nu}^*}{(\mathbf{e}_{j_\nu}^*)^\top (\mathbf{I} - \mathbf{P}_{\widehat{A}_{j_\nu}^*}) \mathbf{e}_{j_\nu}^* / (n - |\widehat{A}_{j_\nu}^*|)}, \end{aligned} \quad (15)$$

where the distributions of Lr_ν^* given \mathbf{Z} approximates the null distributions of Lr_ν . Finally, define the p-value of pathway test in (3) as

$$\text{Pval} = \max_{1 \leq \nu \leq |\mathcal{H}|} \left(\sum_{m=1}^M \mathbf{I}(Lr_{\nu,m}^* \geq Lr_\nu, \widehat{S}_m^* \supseteq \widehat{S}) \right) / \left(\sum_{i=1}^M \mathbf{I}(\widehat{S}_m^* \supseteq \widehat{S}) \right). \quad (16)$$

Note that if any $H_{0,\nu}$ is degenerate, then $\text{Pval} = 1$.

Algorithm 3 summarizes the DP method for hypothesis testing.

Algorithm 3: DP likelihood ratio test

- 1 Specify the Monte Carlo size M .
 - 2 Compute Lr and $\widehat{\boldsymbol{\Sigma}} = \text{Diag}(\widehat{\sigma}_1^2, \dots, \widehat{\sigma}_p^2)$ via Algorithm 2 with original data \mathbf{Z} .
 - 3 (Parallel DP) Generate perturbed data $(\mathbf{Z}_m^*, \mathbf{e}_m^*) = (\mathbf{X}, \mathbf{Y}_m^*, \mathbf{e}_m^*)$ in parallel, where $\boldsymbol{\varepsilon}_{m,i}^* \sim N(\mathbf{0}, \widehat{\boldsymbol{\Sigma}})$. For (2), compute Lr_m^* based on $(\mathbf{Z}_m^*, \mathbf{e}_m^*)$, while, for (3), compute $Lr_{\nu,m}^*$; $\nu = 1, \dots, |\mathcal{H}|$ based on $(\mathbf{Z}_m^*, \mathbf{e}_m^*)$; $m = 1, \dots, M$.
 - 4 Compute the p-value of a test as (14) or (16) accordingly.
-

Remark 4 (Computation) *To accelerate the computation, we consider a parallelizable procedure in Algorithm 3. In addition, we use the original estimate $\widehat{\boldsymbol{\theta}}$ as a warm-start initialization for the DP estimates, which effectively reduces the computing time.*

Remark 5 (Connection with bootstrap) *One may consider parametric or nonparametric bootstrap for Lr . The parametric bootstrap requires a good initial estimate of (\mathbf{U}, \mathbf{W}) .*

Yet, it is rather challenging to correct the bias of this estimate because of the acyclicity constraint. By comparison, DP does not rely on such an estimate. On the other hand, nonparametric bootstrap resamples the original data with replacement. In a bootstrap sample, only about 63% distinct observations in the original data are used in model selection and fitting, leading to deteriorating performance (Kleiner et al., 2012), especially in a small sample. As a result, nonparametric bootstrap may not well-approximate the distribution of L_r , while DP provides a better approximation of L_r , taking advantage of a full sample.

4. Theory

This section provides the theoretical justification for the proposed methods.

4.1 Convergence and consistency of structure learning

First, we introduce some technical assumptions to derive statistical and computational properties of Algorithms 1 and 2. Let $(\mathbf{Y}, \mathbf{X}) \in \mathbb{R}^{n \times (p+q)}$ be the data matrix. Denote by $\boldsymbol{\zeta}$ a generic vector and $\boldsymbol{\zeta}_A \in \mathbb{R}^{|A|}$ be the projection of $\boldsymbol{\zeta}$ onto coordinates in A . Let $\kappa_j^\circ = \|\mathbf{V}_{\cdot j}^\circ\|_0$ and $\kappa_{\max}^\circ = \max_{1 \leq j \leq p} \kappa_j^\circ$.

Assumption 2 (Restricted eigenvalues) For a constant $c_1 > 0$,

$$\min_{A: |A| \leq 2\kappa_{\max}^\circ} \min_{\{\boldsymbol{\zeta}: \|\boldsymbol{\zeta}_{A^c}\|_1 \leq 3\|\boldsymbol{\zeta}_A\|_1\}} \frac{\|\mathbf{X}\boldsymbol{\zeta}\|_2^2}{n\|\boldsymbol{\zeta}\|_2^2} \geq c_1.$$

Assumption 3 (Interventions) For a constant $c_2 > 0$,

$$\max \left(\max_{1 \leq l \leq q} n^{-1} (\mathbf{X}^\top \mathbf{X})_{ll}, \max_{A: |A| \leq 2\kappa_{\max}^\circ} \max_{1 \leq l \leq |A|} n((\mathbf{X}_A^\top \mathbf{X}_A)^{-1})_{ll} \right) \leq c_2^2.$$

Assumption 4 (Nuisance signals)

$$\min_{V_{lj}^0 \neq 0} |V_{lj}^0| \geq 100 \frac{c_2}{c_1} \max_{1 \leq j \leq p} \sqrt{\Omega_{jj}^{-1} \left(\frac{\log(q)}{n} + \frac{\log(n)}{n} \right)}. \quad (17)$$

Assumptions 2-3, as a replacement of Assumption 1A, are satisfied with a probability tending to one for isotropic subgaussian or bounded \mathbf{X} (Rudelson and Zhou, 2012). Assumption 2 is a common condition for proving the convergence rate of Lasso regression (Bickel et al., 2009; Zhang et al., 2014). Assumption 4, as an alternative to Assumption 1B, specifies the minimal signal strength over candidate interventions. A signal strength requirement like Assumption 4 is a condition for establishing selection consistency in high dimensional variable selection (Fan et al., 2014; Loh et al., 2017; Zhao et al., 2018). Moreover, Assumption 4 can be further relaxed to a less intuitive condition, Assumption 6; see Appendix A.3 for details.

Theorem 4 (Finite termination and consistency) Under Assumptions 1-4 with constants $c_1 < 6c_2$, if the machine precision $\text{tol} \ll 1/n$ is negligible, and tuning parameters of Algorithm 1 satisfy:

$$(1) \gamma_j \leq c_1/6,$$

$$(2) \sqrt{32c_2^2\Omega_{jj}^{-1}(\log(q) + \log(n))/n}/\gamma_j \leq \tau_j \leq 0.4 \min_{V_{lj}^0 \neq 0} |V_{lj}^0|,$$

$$(3) \kappa_j = \kappa_j^\circ,$$

for $j = 1, \dots, p$, then Algorithm 1 yields the global minimizer $\widehat{\mathbf{V}}_j$ of (7) in at most $1 + \lceil \log(\kappa_{\max}^\circ)/\log 4 \rceil$ DC iterations almost surely, where $\lceil \cdot \rceil$ is the ceiling function. Moreover, Algorithm 2 recovers \mathcal{A}° , $\mathcal{C}^\circ \equiv \{l : V_{lj}^\circ \neq 0\} \supseteq \mathcal{I}^\circ$, and \mathcal{D}° almost surely as $n \rightarrow \infty$.

By Theorem 4 (proved in Appendix B.4), the computational complexity of Algorithm 1 is the number of iterations multiplied by that of solving a weighted Lasso regression, $O(\log \kappa_{\max}^\circ) \times O(q^3 + nq^2)$ (Efron et al., 2004). Also note that in Steps 2-6 of Algorithm 2, no heavy computation is involved. Thus, the overall time complexity of Algorithm 2 is bounded by $O(p \times \log \kappa_{\max}^\circ \times (q^3 + nq^2))$ for computing $\widehat{\mathbf{V}}$ matrix. Finally, the peeling algorithm does not apply to observational data ($\mathbf{W} = \mathbf{0}$). In a sense, interventions play an essential role.

Although Theorem 4 establishes the consistent reconstruction of the peeling algorithm for the super-graph S , it does not provide any uncertainty measure of the presence of some directed edges of the true DAG. In what follows, we will develop a theory for hypothesis tests to make valid inference concerning directed edges of interest.

4.2 Inferential theory

Assumption 5 (Hypothesis-specific dimension restriction) For a constant ρ ,

$$\max_{j: \mathcal{D}_{G^\circ}(j) \neq \emptyset} \frac{|\text{ANG}^\circ(j)| + |\text{DG}^\circ(j)| + \kappa_j^\circ}{n} \leq \rho < 1, \quad \text{as } n \rightarrow \infty.$$

Assumption 5 is a hypothesis-specific condition restricting the underlying dimension of the testing problem. Usually, $|\text{ANG}^\circ(j)| \asymp \kappa_j^\circ \ll p$; $j = 1, \dots, p$, which dramatically relaxes the condition $n \gg |\mathcal{D}|^{1/2} p \log(p)$ for the constrained likelihood ratio test (Li et al., 2019).

Theorem 5 (Empirical p-values) Suppose Assumptions 1-5 are met and H_0 is regular. If the tuning parameters in Algorithm 1 satisfy (1)-(3) in Theorem 4, then,

(A) (Test of directed edges (2))

$$\begin{aligned} \lim_{\substack{n \rightarrow \infty \\ \theta^\circ \text{ satisfies } H_0 \text{ in (2)}}} \lim_{M \rightarrow \infty} \mathbb{P}_{\theta^\circ}(\text{Pval} < \alpha) &= \alpha, \quad \text{if } H_0 \text{ is nondegenerate;} \\ \lim_{\substack{n \rightarrow \infty \\ \theta^\circ \text{ satisfies } H_0 \text{ in (2)}}} \lim_{M \rightarrow \infty} \mathbb{P}_{\theta^\circ}(\text{Pval} = 1) &= 1, \quad \text{if } H_0 \text{ is degenerate.} \end{aligned}$$

(B) (Test of directed pathways (3))

$$\begin{aligned} \limsup_{\substack{n \rightarrow \infty \\ \theta^\circ \text{ satisfies } H_0 \text{ in (3)}}} \lim_{M \rightarrow \infty} \mathbb{P}_{\theta^\circ}(\text{Pval} < \alpha) &= \alpha, \quad \text{if } H_0 \text{ is nondegenerate with } |\mathcal{D}| = |\mathcal{H}|; \\ \limsup_{\substack{n \rightarrow \infty \\ \theta^\circ \text{ satisfies } H_0 \text{ in (3)}}} \lim_{M \rightarrow \infty} \mathbb{P}_{\theta^\circ}(\text{Pval} = 1) &= 1, \quad \text{if } |\mathcal{D}| < |\mathcal{H}|. \end{aligned}$$

By Theorem 5, the DP likelihood ratio test yields a valid p-value for (2) and (3). Note that $|\mathcal{D}|$ is permitted to depend on n . Moreover, Proposition 6 summarizes the asymptotics for directed edge test (2).

Proposition 6 (Asymptotic distribution of Lr of (2)) *Assume that the assumptions of Theorem 5 are met. Under a regular H_0 , as $n \rightarrow \infty$,*

$$\begin{aligned} 2\text{Lr} &\xrightarrow{d} \chi_{|\mathcal{D}|}^2, \text{ if } H_0 \text{ is nondegenerate with } |\mathcal{D}| > 0 \text{ being fixed;} \\ \frac{2\text{Lr} - |\mathcal{D}|}{\sqrt{2|\mathcal{D}|}} &\xrightarrow{d} N(0, 1), \text{ if } H_0 \text{ is nondegenerate with } |\mathcal{D}| \rightarrow \infty, \frac{|\mathcal{D}| \log |\mathcal{D}|}{n} \rightarrow 0. \end{aligned}$$

The proofs of Theorem 5 and Proposition 6 are given in Appendix B.5 and B.6.

Remark 6 (Local structure for hypothesis testing) *Theorem 5 or Proposition 6 only requires correct identification of the local structures of the DAG such as, $\text{AN}_S(j) = \text{AN}_G(j)$, $\text{D}_S(j) = \text{D}_G(j)$, and $\text{IN}_S(j)$, for variables Y_j with $\text{D}_S(j) \neq \emptyset$, as opposed to those of entire S .*

Next, we analyze the local limit power of the proposed tests for (2) and (3). Assume $\theta^\circ = (\mathbf{U}^\circ, \mathbf{W}^\circ)$ satisfies H_0 . Let $\Delta \in \mathbb{R}^{p \times p}$ satisfy $\Delta_{\mathcal{D}^c} = \mathbf{0}$ so that $\mathbf{U}^\circ + \Delta$ represents a DAG. For nondegenerate and regular H_0 , consider an alternative H_a : $\mathbf{U}_{\mathcal{H}} = \mathbf{U}_{\mathcal{H}}^\circ + \Delta_{\mathcal{H}}$, and define the power function as

$$\beta(\theta^\circ, \Delta) = \mathbb{P}_{H_a}(\text{Pval} < \alpha). \quad (18)$$

Proposition 7 (Local power of edge test) *Assume that H_0 is nondegenerate and regular. Let $\|\Delta\|_F = \|\Delta_{\mathcal{H}}\|_F = n^{-1/2}\delta$ when $|\mathcal{D}| > 0$ is fixed and $\|\Delta\|_F = |\mathcal{D}|^{1/4}n^{-1/2}h$ when $|\mathcal{D}| \rightarrow \infty$, where $\delta > 0$ and $\|\cdot\|_F$ is the matrix Frobenius norm. If the assumptions of Theorem 5 are met, then under H_a , as $n, M \rightarrow \infty$,*

$$\beta(\theta^\circ, \Delta) \geq \begin{cases} \mathbb{P}\left(\|\mathbf{Z} + c_l \sqrt{n} \Delta\|_2^2 > \chi_{|\mathcal{D}|, 1-\alpha}^2\right) & \text{if } |\mathcal{D}| > 0 \text{ is fixed;} \\ \mathbb{P}\left(Z > z_{1-\alpha} - c_l \|\Delta\|_2^2 / \sqrt{2|\mathcal{D}|}\right) & \text{if } |\mathcal{D}| \rightarrow \infty, \frac{|\mathcal{D}| \log |\mathcal{D}|}{n} \rightarrow 0, \end{cases}$$

where $\mathbf{Z} \sim N(\mathbf{0}, \mathbf{I}_{|\mathcal{D}|})$, $Z \sim N(0, 1)$, and $\chi_{|\mathcal{D}|, 1-\alpha}^2$ and $z_{1-\alpha}$ are the $(1-\alpha)$ th quantile of distributions $\chi_{|\mathcal{D}|}^2$ and $N(0, 1)$, respectively. In particular, $\lim_{\delta \rightarrow \infty} \lim_{n \rightarrow \infty} \beta(\theta^\circ, \Delta) = 1$.

Proposition 8 (Local power of pathway test) *Assume that H_0 is nondegenerate and regular with $|\mathcal{D}| = |\mathcal{H}|$. Let $\min_{(k,j) \in \mathcal{H}} |U_{kj}^\circ + \Delta_{kj}| = n^{-1/2}\delta$ when $|\mathcal{H}| > 0$ is fixed and $\min_{(k,j) \in \mathcal{H}} |U_{kj}^\circ + \Delta_{kj}| = n^{-1/2}\delta \sqrt{\log |\mathcal{H}|}$ when $|\mathcal{H}| \rightarrow \infty$. If the assumptions of Theorem 5 are met, then under H_a , as $n, M \rightarrow \infty$,*

$$\beta(\theta^\circ, \Delta) \geq 1 - \frac{|\mathcal{H}|}{\sqrt{2\pi}} \exp\left(-\left(\delta \sqrt{\log |\mathcal{H}|} / \max_{1 \leq j \leq p} \Omega_{jj} - \sqrt{\chi_{1, 1-\alpha}^2}\right)^2 / 2\right),$$

where $Z \sim N\left(\delta^2 / \max_{1 \leq j \leq p} \Omega_{jj}, 1\right)$ and $\chi_{1, 1-\alpha}^2$ is the $(1-\alpha)$ th quantile of distribution χ_1^2 . Then, $\lim_{\delta \rightarrow \infty} \lim_{n \rightarrow \infty} \beta(\theta^\circ, \Delta) = 1$.

The proofs of Propositions 7 and 8 are deferred to Appendix B.7 and B.8.

5. Simulations

This section investigates the operating characteristics of the proposed tests and the peeling algorithm via simulations. In simulations, we consider two setups for generating $\mathbf{U} \in \mathbb{R}^{p \times p}$, representing random and hub DAGs, respectively.

- **Random graph.** The upper off-diagonal entries U_{kj} ; $k < j$ are sampled independently from $\{0, 1\}$ according to Bernoulli($1/p$), while other entries are zero. This generates a random graph with a sparse neighborhood.
- **Hub graph.** Set $U_{1,2j+1} = 1$ and $U_{2,2j+2} = 1$ for $j = 1, \dots, \lfloor p/2 \rfloor - 2$, while other entries are zero. This generates a hub graph, where nodes 1 and 2 are hub nodes with a dense neighborhood.

Moreover, we consider three setups for intervention matrix $\mathbf{W} \in \mathbb{R}^{q \times p}$, representing different scenarios. Setups A and B are designed for inference, whereas Setup C in Section 5.2 is designed to compare with the method of Chen et al. (2018) for structure learning. Let $\mathbf{W} = (\mathbf{A}^\top, \mathbf{B}^\top, \mathbf{0}^\top)^\top$, where $\mathbf{A}, \mathbf{B} \in \mathbb{R}^{p \times p}$ and $\mathbf{0} \in \mathbb{R}^{(q-2p) \times p}$.

- **Setup A.** Set $A_{jj} = B_{jj} = B_{j,j+1} = 1$; $j = 1, \dots, p-1$, $A_{pp} = 1$, while other entries of \mathbf{A}, \mathbf{B} are zero. Then, X_1, \dots, X_p are instruments for Y_1, \dots, Y_p , respectively, X_{p+1}, \dots, X_{2p-1} are invalid instruments with two targets, and X_{2p}, \dots, X_q represent inactive interventions.
- **Setup B.** Set $A_{jj} = A_{j,j+1} = B_{jj} = B_{j,j+1} = 1$; $j = 1, \dots, p-1$, $A_{pp} = 1$, while other entries of \mathbf{A}, \mathbf{B} are zero. Here, the only valid instrument is X_p on Y_p , and the other intervention variables either have two targets or are inactive. Importantly, the instrumental sufficiency (Assumption 1C) is not met.

To generate (\mathbf{X}, \mathbf{Y}) for each setup, we sample $\mathbf{X} \sim N(\mathbf{0}, \Sigma_X)$ with $(\Sigma_X)_{ll'} = 0.5^{|l-l'|}$; $1 \leq l, l' \leq q$ and sample \mathbf{Y} according to (1) with $(\mathbf{U}, \mathbf{W}, \sigma_1^2, \dots, \sigma_p^2)$, where $\sigma_1^2, \dots, \sigma_p^2$ are set to be equally spaced from 0.5 to 1.

5.1 Inference

We compare three tests in empirical type-I errors and powers in simulated examples, namely, the DP likelihood ratio test (DP-LR) in Algorithm 3, the asymptotic likelihood ratio test (LR), and the oracle likelihood ratio test (OLR). Here LR uses $\text{Lr}(\hat{S}, \hat{\Sigma})$, while OLR uses $\text{Lr}(S^\circ, \hat{\Sigma})$ assuming that the super-graph S° were known in advance. The p-values of LR and OLR are computed via Proposition 6. The implementation details of these tests are in Appendix C.

For the empirical type-I error of a test, we compute the percentage of times rejecting H_0 out of 500 simulations when H_0 is true. For the empirical power of a test, we report the percentage of times rejecting H_0 out of 100 simulations when H_a is true under alternative hypotheses H_a .

- **Test of directed edges.** For (2), we examine two different hypotheses:
 - (i) $H_0 : U_{1,20} = 0$ versus $H_a : U_{1,20} \neq 0$. In this case, $|\mathcal{D}| = 1$.

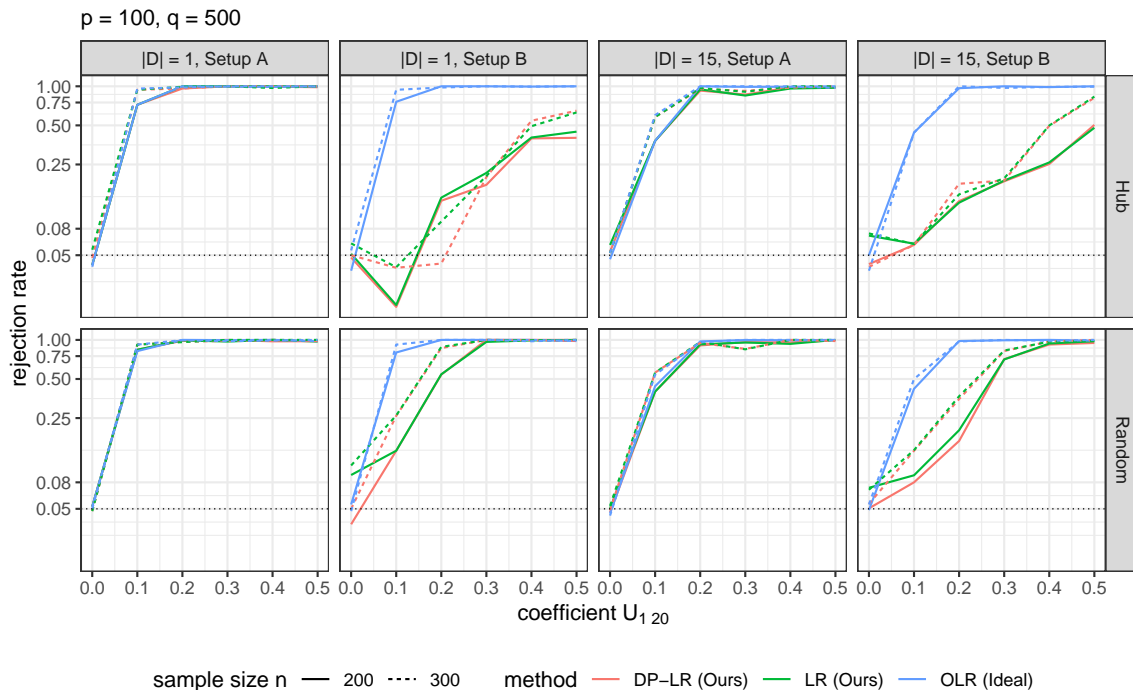


Figure 2: Empirical type-I errors and powers of tests of directed edges. The black dotted line marks the nominal level of significance $\alpha = 0.05$.

(ii) $H_0 : \mathbf{U}_{\mathcal{H}} = \mathbf{0}$ versus $H_a : \mathbf{U}_{\mathcal{H}} \neq \mathbf{0}$, where $\mathcal{H} = \{(k, 20) : k = 1, \dots, 15\}$. In this case, $|\mathcal{D}| = 15$.

Moreover, five alternatives $H_a : U_{1,20} = 0.1l$ and $\mathbf{U}_{\mathcal{H} \setminus \{(1,20)\}} = \mathbf{0}$; $l = 1, 2, 3, 4, 5$, are used for the power analysis in (i) and (ii). The data are generated by modifying \mathbf{U} accordingly.

- **Test of directed pathways.** We examine the test of a directed path $Y_1 \rightarrow Y_5 \rightarrow Y_{10} \rightarrow Y_{15} \rightarrow Y_{20}$, namely $\mathcal{H} = \{(1, 5), (5, 10), (10, 15), (15, 20)\}$ in (3). Since (3) is a test of composite null hypothesis, the data are generated under a graph with parameters $(\mathbf{U}, \mathbf{W}, \mathbf{\Sigma})$ satisfying H_0 , where $\mathbf{U}_{\mathcal{H}} = \mathbf{0}$. Five alternatives $H_a : \mathbf{U}_{\mathcal{H}} = \mathbf{0.1}l$; $l = 1, 2, 3, 4, 5$ are used for the power analysis.

For testing directed edges, as displayed in Figure 2, DP-LR and LR perform well compared to the ideal test OLR in Setup A with Assumption 1 satisfied. In setup B with Assumption 1C not fulfilled, DP-LR appears to have control of type-I error, whereas LR has an inflated empirical type-I error compared to the nominal level $\alpha = 0.05$. This discrepancy is attributed to the data perturbation scheme accounting for the uncertainty of identifying S . However, both suffer a loss of power compared to the oracle test OLR in this setup. This observation suggests that without Assumption 1C, the peeling algorithm tends to yield an estimate $\hat{S} \supseteq S^\circ$, which overestimates S° , resulting in a power loss.

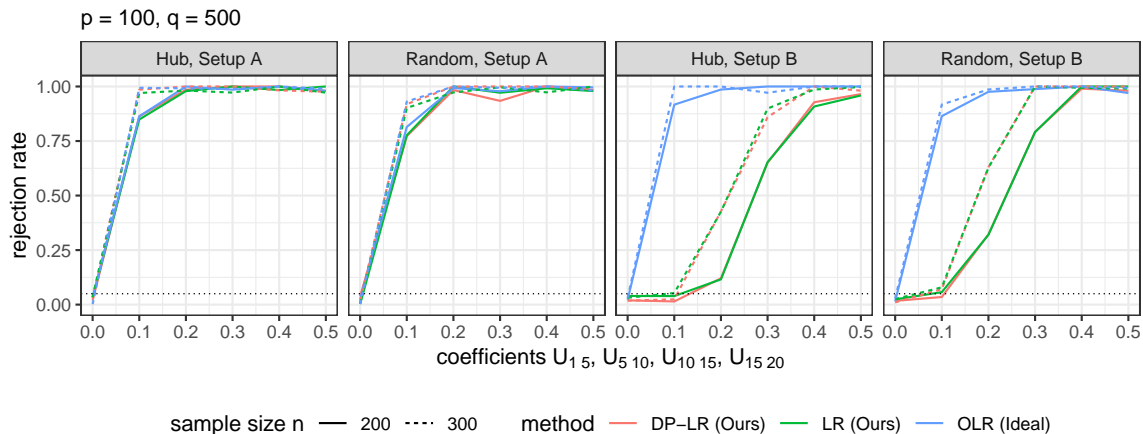


Figure 3: Empirical type-I errors and powers of tests of a directed pathway. The black dotted line marks the nominal level of significance $\alpha = 0.05$.

For testing directed pathways, as indicated in Figure 3, we observe similar phenomena as in the previous directed edge tests. Of note, both LR and DP-LR are capable in controlling type-I error of directed path tests.

In summary, DP-LR has a suitable control of type-I error when there are invalid instruments and Assumption 1C is violated. Concerning the power, DP-LR and LR are comparable in all scenarios and their powers tend to one as the sample size n or the signal strength of tested edges increases. Moreover, DP-LR and LR perform nearly as well as the oracle test OLR when Assumption 1 is satisfied. These empirical findings agree with our theoretical results.

5.2 Structure learning

This subsection compares the peeling algorithm with the Two-Stage Penalized Least Squares (2SPLS, Chen et al. (2018)) in terms of the structure learning accuracy. For peeling, we consider Algorithm 2 with an additional step (9) for structure learning of \mathbf{U} . For 2SPLS, we use the R package `BigSEM`.

2SPLS requires that all the intervention variables to be target-known instruments in addition to Assumption 1C. Thus, we consider an additional Setup C.

- **Setup C.** Let $\mathbf{W} = (\mathbf{I}_{p \times p}, \mathbf{0})^\top \in \mathbb{R}^{q \times p}$. Then X_1, \dots, X_p are valid instruments for Y_1, \dots, Y_p , respectively, and other intervention variables are inactive.

For 2SPLS, we assign each active intervention variable to its most correlated primary variable in Setups A-C. In Setup C, this assignment yields a correct identification of valid instruments, meeting all the requirements of 2SPLS.

For each scenario, we compute the average structural Hamming distance $\text{SHD}(\hat{\mathbf{U}}, \mathbf{U}^\circ) = \sum_{k,j} |\mathbb{I}(\hat{U}_{kj} \neq 0) - \mathbb{I}(U_{kj}^\circ \neq 0)|$ over 100 runs. As shown in Figure 4, the peeling algorithm outperforms 2SPLS, especially when there are invalid instruments and Assumption 1C is violated.

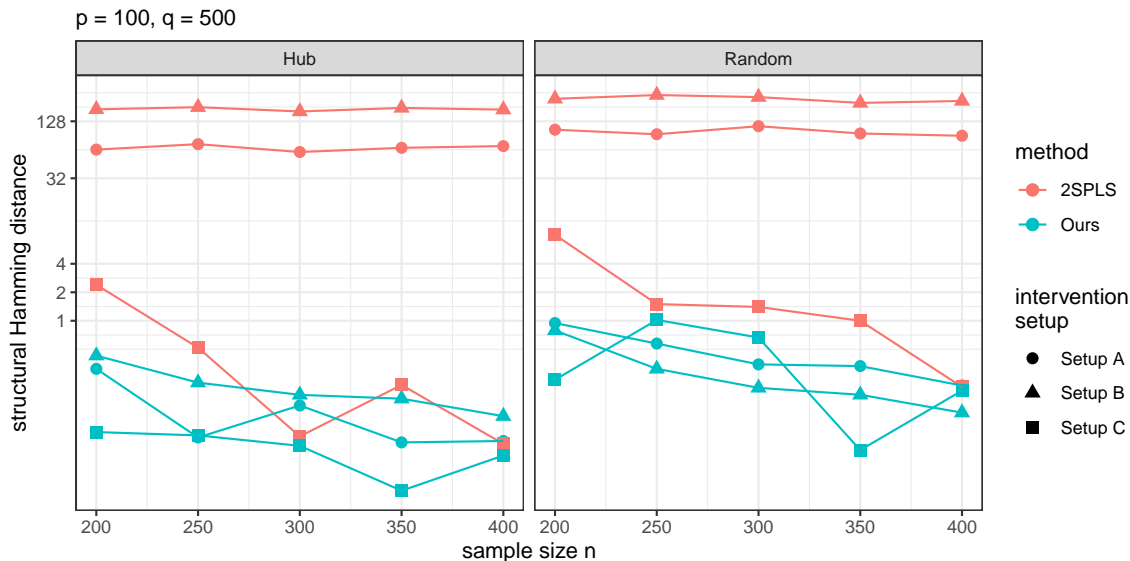


Figure 4: Structural Hamming distances (SHDs) for the peeling algorithm and 2SPLS, where a smaller value of SHD indicates a better result.

5.3 Comparison of inference and structure learning

This subsection compares the proposed DP testing method against the proposed structure learning method in (9) in terms of inferring the true graph structure. To this end, we consider Setup A in Section 5.1 with $p = 30, q = 100$, and the hypotheses

$$H_0 : U_{1,20} = 0 \text{ versus } H_a : U_{1,20} = 1/\sqrt{n}.$$

For DP inference, we use $\alpha = 0.05$ and choose the tuning parameters by BIC as in previous experiments; see Appendix C for details. For structure learning, we reject the null hypothesis when $\hat{U}_{1,20} \neq 0$.

As displayed in Figure 5, when the null hypothesis H_0 is true, the DP testing method controls type-I error very close to the nominal level of 0.05, whereas the type-I error of the structure learning varies greatly depending on the tuning parameter selection. Under the alternative hypothesis H_a , the DP inference enjoys high statistical power than structure learning methods when $n \geq 200$. Interestingly, the power of structure learning diminishes as n increases. This observation is in agreement with our theoretical results in Theorem 4, suggesting that consistent reconstruction requires the smallest size of nonzero coefficients to be of order $\sqrt{\log(n)/n}$ with the tuning parameter τ of the same order (fixing p, q). In this case, the edge $U_{1,20}$ is of order $1/\sqrt{n}$, which is less likely to be reconstructed as n increases. In contrast, Proposition 7 indicates that a DP test has a non-vanishing power when the hypothesized edges are of order $1/\sqrt{n}$.

Figure 5 demonstrates some important distinctions between inference and structure learning. When different tuning parameters are used, the structure learning results correspond to different points on an ROC curve. Although it is asymptotically consistent when optimal tuning parameters are used, structure learning lacks an uncertainty measure of

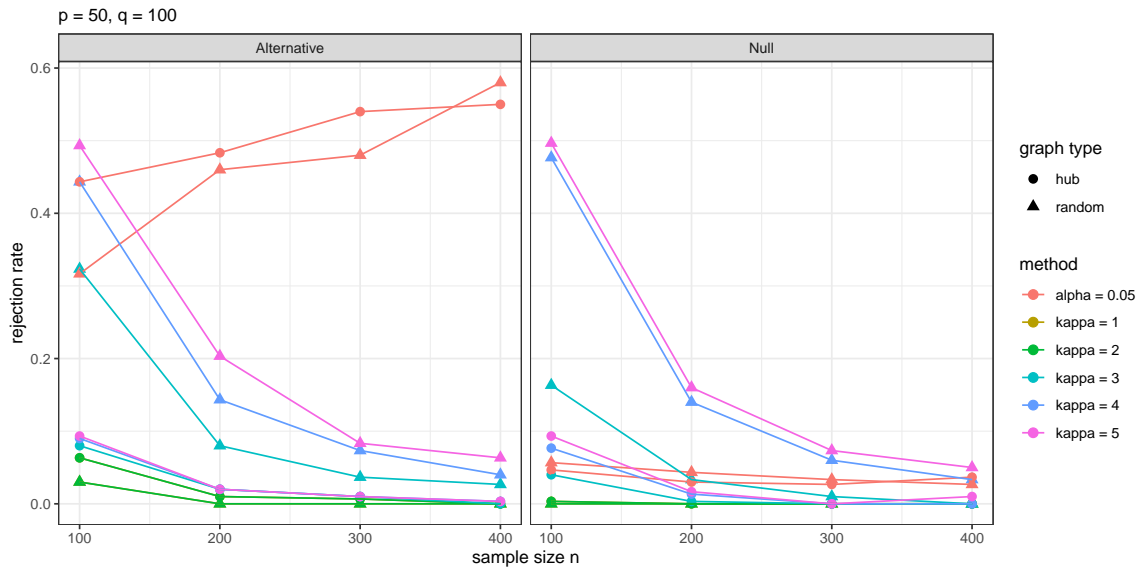


Figure 5: Rejection rates for $H_0 : U_{1,20} = 0$ versus $H_a : U_{1,20} = 1/\sqrt{n}$ by DP inference and structure learning. For structure learning, H_0 is rejected if $\hat{U}_{1,20} \neq 0$. The red lines indicate the results of DP inference using the significance level $\alpha = 0.05$. The other colored lines display the results of structure learning using different sparsity parameter values $\kappa = 1, 2, 3, 4, 5$. The simulation is repeated for 500 times and $\kappa = 2$ is chosen by BIC in over 90% cases.

graph structure identification. As a result, it is nontrivial for structure learning methods to trade-off the false discovery rate and detection power in practice. This makes the interpretation of such results hard, especially when they heavily rely on hyperparameters as in Figure 5. By comparison, DP inference aims to maximize statistical power while controlling type-I error at a given level, offering a clear interpretation of its result. This observation agrees with the discussions in the literature on variable selection and inference (Wasserman and Roeder, 2009; Meinshausen and Bühlmann, 2010; Lockhart et al., 2014; Candès et al., 2018) and it justifies the demand for inferential tools for directed graphical models.

6. ADNI data analysis

This section applies the proposed tests to analyze an Alzheimer’s Disease Neuroimaging Initiative (ADNI) dataset. In particular, we infer gene pathways related to Alzheimer’s Disease (AD) to highlight some gene-gene interactions differentiating patients with AD/cognitive impairments and healthy individuals.

The raw data are available in the ADNI database (<https://adni.loni.usc.edu>), including gene expression, whole-genome sequencing, and phenotypic data. After cleaning and merging, we have a sample size of 712 subjects. From the KEGG database (Kanehisa and Goto, 2000), we extract the AD reference pathway (hsa05010, <https://www.genome.jp/pathway/hsa05010>), including 146 genes in the ADNI data.

For data analysis, we first regress the gene expression levels on five covariates – gender, handedness, education level, age, and intracranial volume, and then use the residuals as gene expressions in the following analysis. Next, we extract the genes with at least one SNP at a marginal significance level below 10^{-3} , yielding $p = 63$ genes as primary variables. For these genes, we further extract their marginally most correlated two SNPs, resulting in $q = 63 \times 2 = 126$ SNPs as unspecified intervention variables, in subsequent data analysis. All gene expression levels are normalized.

The data contains individuals in four groups, namely, Alzheimer’s Disease (AD), Early Mild Cognitive Impairment (EMCI), Late Mild Cognitive Impairment (LMCI), and Cognitive Normal (CN). For our purpose, we treat 247 CN individuals as controls while the remaining 465 individuals as cases (AD-MCI). Then, we use the gene expressions and the SNPs to reconstruct the ancestral relations and infer gene pathways for 465 AD-MCI and 247 CN control cases, respectively.

In the literature, genes APP, CASP3, and PSEN1 are well-known to be associated with AD, reported to play different roles in AD patients and healthy subjects (Julia and Goate, 2017; Su et al., 2001; Kelleher and Shen, 2017). For this dataset, we conduct hypothesis testing on edges and pathways related to genes APP, CASP3, and PSEN1 in the KEGG AD reference (hsa05010) to evaluate the proposed DP inference by checking if DP inference can discover the differences that are reported in the biomedical literature. First, we consider testing $H_0 : U_{kj} = 0$ versus $H_a : U_{kj} \neq 0$, for each edge (k, j) as shown in Figure 6 (a) and (b). Moreover, we consider two hypothesis tests of pathways $H_0 : U_{kj} = 0$ for some $(k, j) \in \mathcal{P}_\ell$ versus $H_a : U_{kj} \neq 0$ for all $(k, j) \in \mathcal{P}_\ell$; $\ell = 1, 2$, where the two pathways are specified by $\mathcal{P}_1 = \{\text{PSEN1} \rightarrow \text{CAPN1} \rightarrow \text{CDK5R1}\}$, and $\mathcal{P}_2 = \{\text{PSEN1} \rightarrow \text{CAPN2} \rightarrow \text{CDK5R1}\}$. See Figure 7. Of note, for clear visualization, Figure 6 (a), (b) and Figure 7 only display the edges related to hypothesis testing, whereas

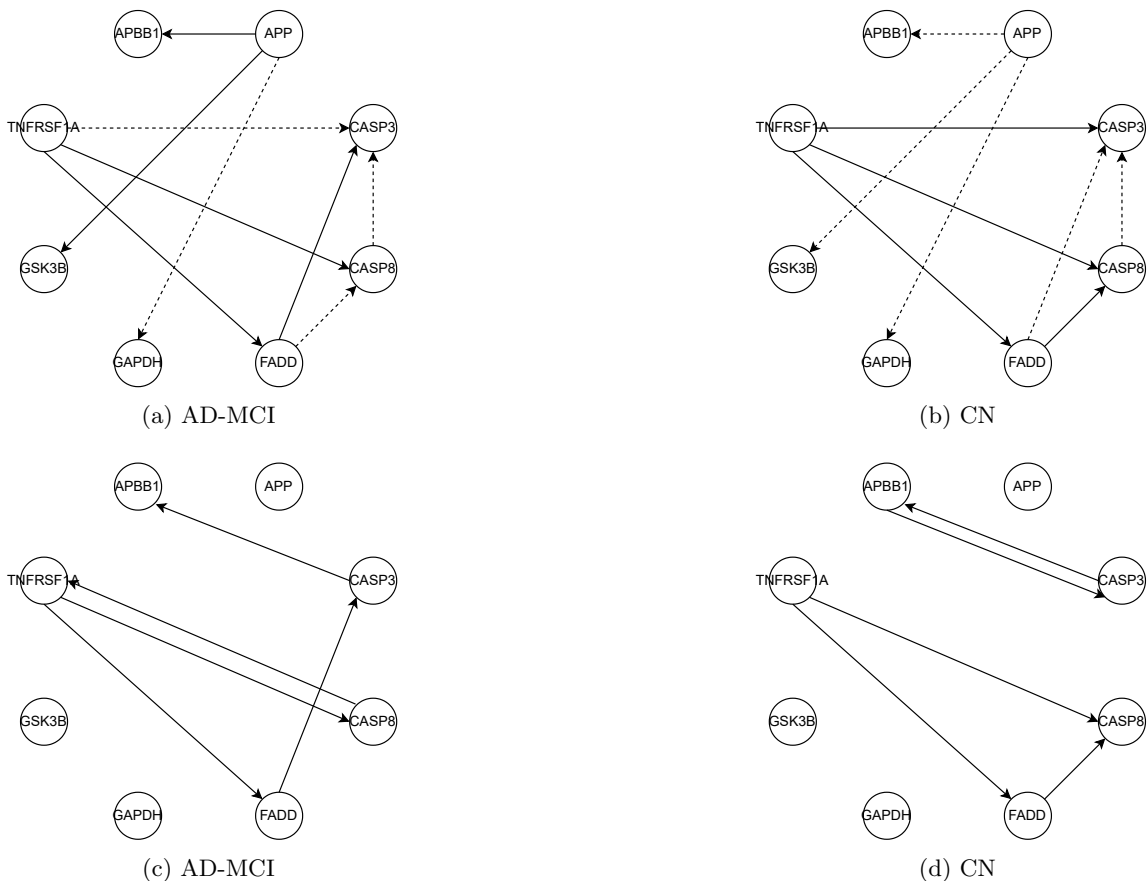


Figure 6: Display of the subnetworks associated with genes APP and CASP3. (a) and (b): Solid/dashed arrows indicate significant/insignificant edges at $\alpha = 0.05$ after adjustment for multiplicity by the Bonferroni-Holm correction. (c) and (d): Solid arrows indicate the reconstructed edges using 2SPLS (Chen et al., 2018).



Figure 7: The p-values of pathway tests (3) by the proposed tests for the AD-MCI and CN groups, where p-values are adjusted for multiplicity by the Bonferroni-Holm correction and solid/dashed arrows indicate significant/insignificant pathways at $\alpha = 0.05$.

the ancestral relations are reconstructed using $p = 63$ genes and $q = 126$ SNPs for AD-MCI and CN groups separately.

In Figures 6-7, the significant results under the level $\alpha = 0.05$ after the Holm-Bonferroni adjustment for $2 \times (9 + 2) = 22$ tests are displayed. In Figures 6, the edge test in (2) exhibits a strong evidence for the presence of directed connectivity $\{\text{APP} \rightarrow \text{APBB1}, \text{APP} \rightarrow \text{GSK3B}, \text{FADD} \rightarrow \text{CASP3}\}$ in the AD-MCI group, but no evidence in the CN group. Meanwhile, this test suggests the presence of connections $\{\text{TNFRSF1A} \rightarrow \text{CASP3}, \text{FADD} \rightarrow \text{CASP8}\}$ in the CN group but not so in the AD-MCI group. In both groups, we identify directed connections $\{\text{TNFRSF1A} \rightarrow \text{FADD}, \text{TNFRSF1A} \rightarrow \text{CASP8}\}$. In Figure 7, the pathway test (3) supports the presence of a pathway $\text{PSEN1} \rightarrow \text{CAPN1} \rightarrow \text{CDK5R1}$ in the AD-MCI group with a p-value of 0.044 but not in the CN group with a p-value of 0.33. The pathway $\text{PSEN1} \rightarrow \text{CAPN2} \rightarrow \text{CDK5R1}$ appears insignificant at $\alpha = 0.05$ for both groups. Also noted is that some of our discoveries agree with the literature according to the AlzGene database (alzgene.org) and the AlzNet database (<https://mips.helmholtz-muenchen.de/AlzNet-DB>). Specifically, GSK3B differentiates AD patients from normal subjects; as shown in Figures 6, our result indicates the presence of connection $\text{APP} \rightarrow \text{GSK3B}$ for the AD-MCI group, but not for the CN group, the former of which is confirmed by Figure 1 of Vanleuven (2011). The connection $\text{APP} \rightarrow \text{APBB1}$ also differs in AD-MCI and CN groups, which appears consistent with Figure 3 of Bu (2009). Moreover, the connection $\text{CAPN1} \rightarrow \text{CDK5R1}$, in the pathway $\text{PSEN1} \rightarrow \text{CAPN1} \rightarrow \text{CDK5R1}$ discovered in AD-MCI group, is found in the AlzNet database (interaction-ID 24614, <https://mips.helmholtz-muenchen.de/AlzNet-DB/entry/show/1870>). Finally, as suggested by Figure 8, the normality assumption in (1) is adequate for both groups.

By comparison, as shown in Figure 6 (c) and (d), gene APP in the reconstructed networks by 2SPLS (Chen et al., 2018) is not connected with other genes, indicating no regulatory relation of APP with other genes in the AD-MCI and CN groups. However, as a well-known gene associated with AD, APP is reported to play different roles in controlling the expressions of other genes for AD patients and healthy people (Matsui et al., 2007; Julia and Goate, 2017). Our results in Figure 6 (a) and (b) are congruous with the studies: the connections of APP with other genes are different in our estimated networks for AD-MCI and CN groups.

In summary, our findings seem to agree with those in the literature (Julia and Goate, 2017; Su et al., 2001; Kelleher and Shen, 2017), where the subnetworks of genes APP, CASP3 in Figure 6 and PSEN1 in Figure 7 differentiate the AD-MCI from the CN groups. Furthermore, the pathway $\text{PSEN1} \rightarrow \text{CAPN1} \rightarrow \text{CDK5R1}$ in Figure 7 seems to differentiate these groups, which, however, requires validation in biological experiments.

7. Summary

This article proposes structure learning and inference methods for a Gaussian DAG with interventions, where the targets and strengths of interventions are unknown. A likelihood ratio test is derived based on an estimated super-graph formed by ancestral relations and candidate interventional relations. This test accounts for the statistical uncertainty of the construction of the super-graph based on a novel data perturbation scheme. Moreover, we develop a peeling algorithm for the super-graph construction. The peeling algorithm allows

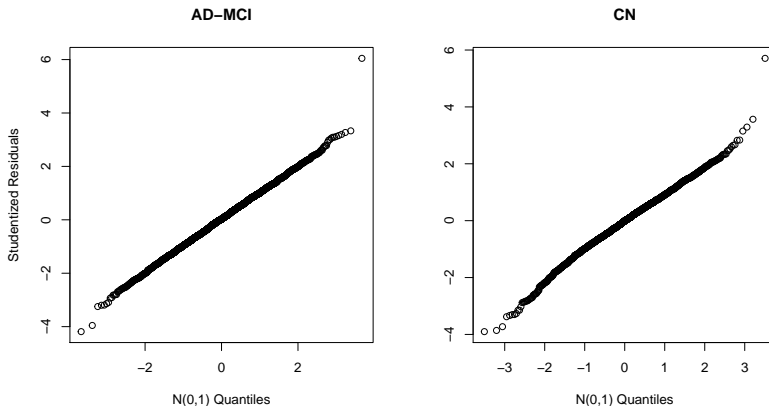


Figure 8: Normal quantile-quantile plots of studentized residuals of the AD-MCI and CN groups.

scalable computing and yields a consistent estimator. The numerical studies justify our theory and demonstrate the utility of our methods.

The proposed methods can be extended to many practical situations beyond biological applications with independent and identically distributed data. An instance is to infer directed relations between multiple autoregressive time series (Pamfil et al., 2020), where the lagged variables and covariates can serve as interventions for each time series.

Acknowledgments

The authors would like to thank the action editor and anonymous referees for helpful comments and suggestions. The research is supported by NSF grants DMS-1712564, DMS-1952539 and NIH grants R01GM126002, R01HL116720, R01HL105397, R01AG069895, R01AG065636, R01AG074858, and U01AG073079.

Appendix A. Illustrative examples and discussions

A.1 Identifiability of model (1) and Assumption 1

The parameter space for model (1) is

$$\{(U, W, \Sigma) : U \in \mathbb{R}^{p \times p} \text{ represents a DAG, } W \in \mathbb{R}^{p \times q}, \Sigma = \text{diag}(\sigma_1^2, \dots, \sigma_p^2)\}.$$

As suggested by Proposition 1, Assumption 1 (1A-1C) suffices for identification of every parameter value in the parameter space. Next, we show by examples that if Assumption 1B or 1C is violated then model (1) is no longer identifiable.

Before proceeding, we rewrite (1) as

$$Y = V^\top X + \varepsilon_V, \quad \varepsilon_V = (I - U^\top)^{-1} \varepsilon \sim N(\mathbf{0}, \Omega^{-1}),$$

where $\Omega = (I - U)\Sigma^{-1}(I - U^\top)$ is a precision matrix and $V = W(I - U)^{-1}$.

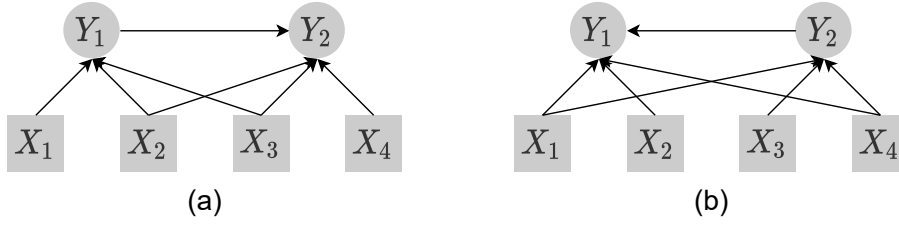


Figure 9: (a) Display of DAG defined by (19). (b) Display of DAG defined by (20).

Example 2 (Identifiability) In model (1), consider two non-identifiable bivariate situations: (1) $p = 2$ and $q = 4$ and (2) $p = 2$ and $q = 2$.

- (1) Model (1) is non-identifiable when Assumption 1B breaks down. Consider two different models with different parameter values:

$$\begin{aligned} \boldsymbol{\theta} : \quad & Y_1 = X_1 + X_2 + X_3 + \varepsilon_1, & Y_2 = Y_1 - X_2 + X_3 + X_4 + \varepsilon_2 & (19) \\ \tilde{\boldsymbol{\theta}} : \quad & Y_1 = 0.5Y_2 + 0.5X_1 + X_2 - 0.5X_4 + \tilde{\varepsilon}_1, & Y_2 = X_1 + 2X_3 + X_4 + \tilde{\varepsilon}_2, & (20) \end{aligned}$$

where $\varepsilon_1, \varepsilon_2 \sim N(0, 1)$ are independent, and $\tilde{\varepsilon}_1 \sim N(0, 0.5)$, $\tilde{\varepsilon}_2 \sim N(0, 2)$ are independent. As depicted in Figure 9, (19) satisfies Assumption 1C. However, Assumption 1B is violated given that $\text{Cov}(Y_2, X_2 \mid \mathbf{X}_{\{1,3,4\}}) = 0$ and X_2 is an intervention variable of Y_2 . This is because the direct interventional effect of X_2 on Y_2 are canceled out by its indirect interventional effect through Y_1 . Similarly, (20) satisfies Assumption 1C but $\text{Cov}(Y_1, X_4 \mid \mathbf{X}_{\{1,2,3\}}) = 0$ violating Assumption 1B. In this case, it can be verified that $\boldsymbol{\theta}$ and $\tilde{\boldsymbol{\theta}}$ correspond to the same distribution $\mathbb{P}(\mathbf{Y} \mid \mathbf{X})$, because they share the same $(\mathbf{V}, \boldsymbol{\Omega})$ even with different values of $(\mathbf{U}, \mathbf{W}, \boldsymbol{\Sigma})$. Hence, it is impossible to infer the directed relation between Y_1 and Y_2 .

- (2) Model (1) is non-identifiable when Assumption 1C breaks down. Consider two different models with different parameter values:

$$\boldsymbol{\theta} : \quad Y_1 = X_1 + X_2 + \varepsilon_1, \quad Y_2 = Y_1 + X_2 + \varepsilon_2, \quad (21)$$

$$\tilde{\boldsymbol{\theta}} : \quad Y_1 = 0.5Y_2 + 0.5X_1 + \tilde{\varepsilon}_1, \quad Y_2 = X_1 + 2X_2 + \tilde{\varepsilon}_2, \quad (22)$$

where $\varepsilon_1, \varepsilon_2 \sim N(0, 1)$ are independent, and $\tilde{\varepsilon}_1 \sim N(0, 0.5)$, $\tilde{\varepsilon}_2 \sim N(0, 2)$ are independent. Note that (21) and (22) satisfy Assumption 1B. In (21), Y_2 does not have any instrumental intervention although it has an invalid instrument X_2 . Similarly, in (22), neither does Y_1 have any instrumental intervention while having an invalid instrument X_1 . As in the previous case, $\boldsymbol{\theta}$ and $\tilde{\boldsymbol{\theta}}$ yield the same distribution $\mathbb{P}(\mathbf{Y} \mid \mathbf{X})$ because they share the same $(\mathbf{V}, \boldsymbol{\Omega})$ even with different values of $(\mathbf{U}, \mathbf{W}, \boldsymbol{\Sigma})$. In this case, it is impossible to infer the directed relation between Y_1 and Y_2 .

A.2 Illustration of Algorithm 2

We now illustrate Algorithm 2 by Example 3.

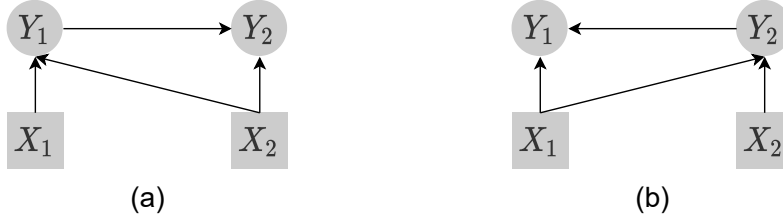


Figure 10: (a) Display of DAG defined by (21). (b) Display of DAG defined by (22).

Example 3 Consider model (1) with $p = q = 5$,

$$\begin{aligned} Y_1 &= X_1 + \varepsilon_1, & Y_2 &= 0.5Y_1 + X_3 + \varepsilon_2, & Y_5 &= X_4 + \varepsilon_5, \\ Y_3 &= 0.5Y_2 + X_5 + \varepsilon_3, & Y_4 &= 0.5Y_3 - 0.1Y_1 + X_2 + \varepsilon_4, \end{aligned} \quad (23)$$

where $\varepsilon_1, \dots, \varepsilon_5 \sim N(0, 1)$ are independent. Then (23) defines a DAG as displayed in Figure 1(a). For illustration, we generate a random sample of size $n = 40$ and compute $\hat{\mathbf{V}}$ by Algorithm 1. In particular,

$$\mathbf{V}^\circ = \begin{pmatrix} 1 & 0.5 & 0.25 & 0.025 & 0 \\ 0 & 0 & 0 & 1 & 0 \\ 0 & 1 & 0.5 & 0.25 & 0 \\ 0 & 0 & 0 & 0 & 1 \\ 0 & 0 & 1 & 0.5 & 0 \end{pmatrix}, \quad \hat{\mathbf{V}} = \begin{pmatrix} 0.92 & 0.48 & 0.27 & 0 & 0 \\ 0 & 0 & 0 & 1.08 & 0 \\ 0 & 1.03 & 0.52 & 0.21 & 0 \\ 0 & 0 & 0 & 0 & 1.06 \\ 0 & 0 & 0.98 & 0.55 & 0 \end{pmatrix}.$$

Algorithm 2 proceeds as follows.

- $h = 0$: We have the set $\{X_2, X_4\}$ of instruments on leaves.
 - X_2 is identified as an instrument of leaf node Y_4 ($X_2 \rightarrow Y_4$) as $\hat{V}_{24} \neq 0$ is the only nonzero in the row 2 with the smallest (positive) row ℓ_0 -norm.
 - X_4 is identified as an instrument of leaf node Y_5 ($X_4 \rightarrow Y_5$) as $\hat{V}_{45} \neq 0$ is the only nonzero in row 4 with the smallest (positive) row ℓ_0 -norm.

Then $h_G(4) = h_G(5) = 0$ and $\{Y_4, Y_5\}$ are removed.

- $h = 1$: We have the set $\{X_5\}$ of instrument on leaf.
 - X_5 is identified as an instrument of a leaf node Y_3 ($X_5 \rightarrow Y_3$) in the subgraph for Y_1, Y_2, Y_3 given that $\hat{V}_{53} \neq 0$ is the only nonzero element in the row with the smallest (positive) row ℓ_0 -norm of the submatrix for Y_1, Y_2, Y_3 . Since $\hat{V}_{54} \neq 0$ and $h_G(4) = 0$, we have $Y_3 \rightarrow Y_4$ by Proposition 3.

Then $h_G(3) = 1$ and $\{Y_3\}$ is removed.

- $h = 2$: We have the set $\{X_3\}$ of instrument on leaf.
 - X_3 is identified as an instrument of a leaf node Y_2 ($X_3 \rightarrow Y_2$) similarly in the subgraph for Y_1, Y_2 given that $\hat{V}_{32} \neq 0$ is the largest nonzero element in its row of the submatrix. Since $\hat{V}_{33} \neq 0$ and $h_G(3) = 1$, we have $Y_2 \rightarrow Y_3$.

Then $h_G(2) = 2$ and $\{Y_2\}$ is removed.

- $h = 3$: We have the set $\{X_1\}$ of instrument on leaf.
 - X_1 is an instrument of Y_1 ($X_1 \rightarrow Y_1$). Since $\widehat{V}_{12} \neq 0$ and $h_G(2) = 2$, we have $Y_1 \rightarrow Y_2$.

Then $h_G(1) = 3$, $\{Y_1\}$ is removed, and the peeling process is terminated.

Finally, Step 6 of Algorithm 2 identifies the ancestral relations

$$\widehat{\mathcal{A}} = \{(1, 2), (2, 3), (3, 4), (1, 3), (1, 4), (2, 4)\}$$

and the candidate interventional relations

$$\widehat{\mathcal{I}} = \{(1, 1), (1, 2), (1, 3), (2, 4), (3, 2), (3, 3), (3, 4), (4, 5), (5, 3), (5, 4)\}.$$

In Example 3, $\widehat{\mathbf{V}} \neq \mathbf{V}^\circ$, suggesting that the selection consistency of matrix \mathbf{V}° is unnecessary for Algorithm 2 to correctly reconstruct ancestral relations \mathcal{A}° ; see also Section A.3.

A.3 Relaxation of Assumption 4

Assumption 4 in Theorem 4 leads to consistent identification for \mathbf{V}° . Now, we discuss when Algorithm 2 correctly reconstruct ancestral relations \mathcal{A}° without requiring Assumption 4.

Assumption 6 *There exists (κ_j^*, τ_j^*) such that $\kappa_j^* = |\{l : |V_{lj}^\circ| \geq \tau_j^*\}|$ and*

$$\begin{aligned} & \min \left(\min_{l: X_l \rightarrow Y_j} |V_{lj}^\circ|, \min_{\substack{l: X_l \rightarrow Y_k \rightarrow Y_j \\ \text{with } h(k)=h(j)+1}} |V_{lj}^\circ| \right) \\ & \geq \tau_j^* \geq 100 \frac{c_2}{c_1} \sqrt{\Omega_{jj}^{-1} (\kappa_j^\circ - \kappa_j^* + 1) \left(\frac{\log(q)}{n} + \frac{\log(n)}{n} \right)}; \quad 1 \leq j \leq p. \end{aligned} \tag{24}$$

Assumption 6 requires a subset of nonzero entries in \mathbf{V}° to exceed a certain signal strength. These signals enable us to reconstruct the topological layers and \mathcal{A}° . Note that Assumption 6 reduces to Assumption 4 when $\kappa_j^* = \kappa_j^\circ$.

Theorem 9 *Under Assumptions 1-3 and 6 with constants $c_1 < 6c_2$, if the machine precision $\text{tol} \ll 1/n$ is negligible and tuning parameters of Algorithm 1 satisfy:*

- (1) $\gamma_j \leq c_1/6 \sqrt{\kappa_j^\circ - \kappa_j^* + 1}$,
- (2) $\sqrt{32c_2^2 \Omega_{jj}^{-1} (\log(q) + \log(n)) / n} / \gamma_j \leq \tau_j \leq 0.4\tau_j^*$,
- (3) $\kappa_j = \kappa_j^\circ$,

for $j = 1, \dots, p$, then Algorithm 1 terminates in at most $1 + \lceil \log(\kappa_{\max}^\circ) / \log 4 \rceil$ iterations almost surely. Moreover, $\widehat{\mathcal{A}} = \mathcal{A}^\circ$, $\widehat{\mathcal{C}} \supseteq \{(l, j) : |V_{lj}^\circ| \geq \tau_j^*\} \supseteq \mathcal{I}^\circ$, and $\widehat{\mathcal{D}} = \mathcal{D}^\circ$ almost surely as $n \rightarrow \infty$.

The proof of Theorem 9 is given in Appendix B.9.

A.4 Comparison of strong faithfulness and Assumption 4 (or 6)

In the literature, a faithfulness condition is usually assumed for identifiability up to Markov equivalence classes (Spirtes et al., 2000). For discussion, we formally introduce the concepts of faithfulness and strong faithfulness.

Consider a DAG G with node variables $(Z_1, \dots, Z_{p+q})^\top$. Nodes Z_i and Z_j are adjacent if $Z_i \rightarrow Z_j$ or $Z_j \rightarrow Z_i$. A *path* (undirected) between Z_i and Z_j in G is a sequence of distinct nodes (Z_i, \dots, Z_j) such that all pairs of successive nodes in the sequence are adjacent. A nonendpoint node Z_k on a path $(Z_i, \dots, Z_{k-1}, Z_k, Z_{k+1}, \dots, Z_j)$ is a *collider* if $Z_{k-1} \rightarrow Z_k \leftarrow Z_{k+1}$. Otherwise it is a *noncollider*. Let $A \subseteq \{1, \dots, p+q\}$, where A does not contain i and j . Then \mathbf{Z}_A *blocks* a path (Z_i, \dots, Z_j) if at least one of the following holds: (i) the path contains a noncollider that is in \mathbf{Z}_A , or (ii) the path contains a collider that is not in \mathbf{Z}_A and has no descendant in \mathbf{Z}_A . A node Z_i is d-separated from Z_j given \mathbf{Z}_A if \mathbf{Z}_A block every path between Z_i and Z_j ; $i \neq j$ (Pearl, 2000).

According to Uhler et al. (2013), a multivariate Gaussian distribution of $(Z_1, \dots, Z_{p+q})^\top$ is said to be ς -strong faithful to a DAG with node set $\mathcal{V} = \{1, \dots, p+q\}$ if

$$\min_{A \subseteq \mathcal{V} \setminus \{i, j\}} \left\{ |\text{Corr}(Z_i, Z_j \mid \mathbf{Z}_A)| : Z_i \text{ is not d-separated from } Z_j \text{ given } \mathbf{Z}_A \right\} > \varsigma, \quad (25)$$

for $1 \leq i \neq j \leq p+q$, where $\varsigma \in [0, 1)$, Corr denotes the correlation. When $\varsigma = 0$, (25) is equivalent to faithfulness. For consistent structure learning (up to Markov equivalence classes), it often requires that $\varsigma \gtrsim \sqrt{s_0 \log(p+q)/n}$, where s_0 is a sparsity measure; see Uhler et al. (2013) for a survey. For a pair (i, j) , the number of possible sets for A is $2^{(p+q-2)}$. If $Z_i \rightarrow Z_j$, then $\text{Corr}(Z_i, Z_j \mid \mathbf{Z}_A) \neq 0$ for any A . Therefore, for this (i, j) pair alone, (25) could require exponentially many conditions. Indeed, (25) is very restrictive in high-dimensional situation (Uhler et al., 2013).

By comparison, Algorithm 2 yields consistent structure learning based on Assumption 4 or 6 instead of strong faithfulness. In some sense, Assumption 4 or 6 requires the sufficient signal strength that is analogous to the condition for consistent feature selection (Shen et al., 2012). This assumption may be thought of as an alternative to strong faithfulness. As illustrated in Example 4, Assumption 4 or 6 is less stringent than strong faithfulness.

Example 4 (Faithfulness) *For simplicity, assume $\mathbf{X} \sim N(\mathbf{0}, \mathbf{I})$. Consider model (1) with $p = q = 3$,*

$$Y_1 = W_{11}X_1 + \varepsilon_1, \quad Y_2 = U_{12}Y_1 + W_{22}X_2 + \varepsilon_2, \quad Y_3 = U_{13}Y_1 + U_{23}Y_2 + W_{33}X_3 + \varepsilon_3,$$

where $\varepsilon_1, \varepsilon_2, \varepsilon_3 \sim N(0, 1)$ are independent and $U_{12}, U_{13}, U_{23}, W_{11}, W_{22}, W_{33} \neq 0$. Let $\mathbf{Z} = (Y_1, Y_2, Y_3, X_1, X_2, X_3)^\top$. Since directed relations among \mathbf{X} are not of interest, (25) becomes

$$\begin{aligned} & \min_{\substack{\mathbf{Z}_A = (\mathbf{Y}_{A_1}, \mathbf{X}_{A_2}): \\ A_1 \subseteq \{i, j\}^c, A_2}} \left\{ |\text{Corr}(Y_i, Y_j \mid \mathbf{Z}_A)| : Y_i, Y_j \text{ are not d-separated given } \mathbf{Z}_A \right\} > \varsigma, \\ & \min_{\substack{\mathbf{Z}_A = (\mathbf{Y}_{A_1}, \mathbf{X}_{A_2}): \\ A_1 \subseteq \{j\}^c, A_2 \subseteq \{l\}^c}} \left\{ |\text{Corr}(Y_j, X_l \mid \mathbf{Z}_A)| : Y_j, X_l \text{ are not d-separated given } \mathbf{Z}_A \right\} > \varsigma, \end{aligned} \quad (26)$$

for each pair (i, j) with $i \neq j$ and each pair (l, j) . Then strong-faithfulness in (26) assumes 152 conditions for the correlations. By comparison, (17) requires the absolute values of $V_{11}, V_{12}, V_{13}, V_{22}, V_{23}, V_{33} \gtrsim \sqrt{\log(q)/n}$, which in turn requires the minimal absolute value of six correlations $\gtrsim \sqrt{\log(q)/n}$,

(i) $\text{Corr}(Y_1, X_1 | X_2, X_3)$, (ii) $\text{Corr}(Y_2, X_1 | X_2, X_3)$, (iii) $\text{Corr}(Y_3, X_1 | X_2, X_3)$,
 (iv) $\text{Corr}(Y_2, X_2 | X_1, X_3)$, (v) $\text{Corr}(Y_3, X_2 | X_1, X_3)$, (vi) $\text{Corr}(Y_3, X_3 | X_1, X_2)$.

Importantly, (i)-(vi) are required in (26), suggesting that strong-faithfulness is more stringent than (17).

A.5 Irregular hypothesis

Assume, without loss of generality, that $\widehat{\mathcal{D}} = \mathcal{D}^\circ$ and $\widehat{\mathcal{A}} = \mathcal{A}^\circ$ are correctly reconstructed in the following discussion.

- For testing of directed edges (2), suppose H_0 is irregular, namely, $\mathcal{D}^\circ \cup \mathcal{E}^\circ$ contains a directed cycle. This implies that a directed cycle exists in $\widehat{\mathcal{D}} \cup \widehat{\mathcal{A}}$. In this situation, we decompose H_0 into sub-hypotheses $H_0^{(1)}, \dots, H_0^{(\nu)}$, each of which is regular. Then testing H_0 is equivalent to multiple testing for $H_0^{(1)}, \dots, H_0^{(\nu)}$. For instance, in Example 1, $H_0 : U_{45} = U_{53} = 0$ is irregular, and H_0 can be decomposed into $H_0^{(1)} : U_{45} = 0$ and $H_0^{(2)} : U_{53} = 0$.
- For testing of directed pathways (3), if H_0 is irregular, then $\widehat{\mathcal{D}} \cup \widehat{\mathcal{A}}$ has a directed cycle. The p-value is defined to be one in this situation since no evidence supports the presence of the pathway.

Appendix B. Technical proofs

B.1 Proof of Proposition 1

Suppose that $\boldsymbol{\theta} = (\mathbf{U}, \mathbf{W}, \boldsymbol{\Sigma})$ and $\widetilde{\boldsymbol{\theta}} = (\widetilde{\mathbf{U}}, \widetilde{\mathbf{W}}, \widetilde{\boldsymbol{\Sigma}})$ render the same distribution of (\mathbf{X}, \mathbf{Y}) . We will prove that $\boldsymbol{\theta} = \widetilde{\boldsymbol{\theta}}$.

Denote by $G(\boldsymbol{\theta})$ and $G(\widetilde{\boldsymbol{\theta}})$ the DAGs corresponding to $\boldsymbol{\theta}$ and $\widetilde{\boldsymbol{\theta}}$, respectively. First, consider $G(\boldsymbol{\theta})$. Without loss of generality, assume Y_1 is a leaf node. By Assumption 1C, there exists an instrumental intervention with respect to $G(\boldsymbol{\theta})$, say X_1 . Then,

$$\text{Cov}(Y_j, X_1 | \mathbf{X}_{\{2, \dots, q\}}) = 0, \quad j = 2, \dots, p, \quad (27)$$

$$\text{Cov}(Y_1, X_1 | \mathbf{Y}_A, \mathbf{X}_{\{2, \dots, q\}}) \neq 0, \quad \text{for any } A \subseteq \{2, \dots, p\}. \quad (28)$$

By the local Markov property (Spirtes et al., 2000), (28) implies that $X_1 \rightarrow Y_1$ in $G(\widetilde{\boldsymbol{\theta}})$. Suppose Y_1 is not a leaf node in $G(\widetilde{\boldsymbol{\theta}})$. Assume, without loss of generality, that $Y_1 \rightarrow Y_2$ with $h_{G(\widetilde{\boldsymbol{\theta}})}(1) = h_{G(\widetilde{\boldsymbol{\theta}})}(2) + 1$. Then $\text{Cov}(Y_2, X_1 | \mathbf{X}_{\{2, \dots, q\}}) = 0$ but $X_1 \rightarrow Y_1$ and $Y_1 \rightarrow Y_2$ with $h_{G(\widetilde{\boldsymbol{\theta}})}(1) = h_{G(\widetilde{\boldsymbol{\theta}})}(2) + 1$, which contradicts to Assumption 1B. This implies that if Y_1 is a leaf node in $G(\boldsymbol{\theta})$ then it must be a leaf node in $G(\widetilde{\boldsymbol{\theta}})$. In both $G(\boldsymbol{\theta})$ and $G(\widetilde{\boldsymbol{\theta}})$, the parents and interventions of Y_1 can be identified by

$$\begin{aligned} \mathbb{E}(Y_1 | \mathbf{Y}_{\{2, \dots, p\}}, \mathbf{X}) &= \mathbb{E}(Y_1 | \mathbf{Y}_{\text{PA}_{G(\boldsymbol{\theta})}(1)}, \mathbf{X}) = \mathbb{E}(Y_1 | \mathbf{Y}_{\text{PA}_{G(\boldsymbol{\theta})}(1)}, \mathbf{X}_{\text{IN}_{G(\boldsymbol{\theta})}(1)}), \\ \mathbb{E}(Y_1 | \mathbf{Y}_{\{2, \dots, p\}}, \mathbf{X}) &= \mathbb{E}(Y_1 | \mathbf{Y}_{\text{PA}_{G(\widetilde{\boldsymbol{\theta}})}(1)}, \mathbf{X}) = \mathbb{E}(Y_1 | \mathbf{Y}_{\text{PA}_{G(\widetilde{\boldsymbol{\theta}})}(1)}, \mathbf{X}_{\text{IN}_{G(\widetilde{\boldsymbol{\theta}})}(1)}). \end{aligned}$$

Consequently, Y_1 has the same parents and interventions in $G(\boldsymbol{\theta})$ and $G(\tilde{\boldsymbol{\theta}})$.

The forgoing argument is applied to other nodes sequentially. First, we remove Y_1 with any directed edges to Y_1 , which does not alter the joint distribution of $(\mathbf{Y}_{\{2,\dots,p\}}, \mathbf{X})$ and the subgraph of nodes Y_2, \dots, Y_p . By induction, we remove the leafs in $G(\boldsymbol{\theta})$ until it is empty, leading to $G(\boldsymbol{\theta}) = G(\tilde{\boldsymbol{\theta}})$. Finally, $\boldsymbol{\theta} = \tilde{\boldsymbol{\theta}}$ because they have the same locations for nonzero elements and these model parameters (or regression coefficients) are uniquely determined under Assumption 1A (Shojaie and Michailidis, 2010). This completes the proof.

B.2 Proof of Proposition 2

It follows from Assumption 1B that $\mathcal{C} = \{(l, j) : V_{lj} \neq 0\} \supseteq \mathcal{I}$.

PROOF OF (A)

Note that the maximal length of a path in a DAG of p nodes is at most $p-1$. Then it can be verified that \mathbf{U} is nilpotent in that $\mathbf{U}^p = \mathbf{0}$. An application of the matrix series expansion yields that $(\mathbf{I} - \mathbf{U})^{-1} = \mathbf{I} + \mathbf{U} + \dots + \mathbf{U}^{p-1}$. Using the fact that $\mathbf{V} = \mathbf{W}(\mathbf{I} - \mathbf{U})^{-1}$ from (6), we have, for any $1 \leq l, j \leq p$,

$$V_{lj} = \sum_{k=1}^p W_{lk} \left(I_{kj} + U_{kj} + \dots + (\mathbf{U}^{p-1})_{kj} \right),$$

where U_{kj} is the (k, j) th entry of \mathbf{U} . If $V_{lj} \neq 0$, then there exists k such that $W_{lk} \neq 0$ and $(\mathbf{U}^r)_{kj} \neq 0$ for some $0 \leq r \leq p-1$. If $r = 0$, then we must have $k = j$, and $X_l \rightarrow Y_j$. If $r > 0$, then $X_l \rightarrow Y_k$ and Y_k is an ancestor of Y_j .

PROOF OF (B)

First, for any leaf node variable Y_j , by Assumption 1, there exists an instrument $X_l \rightarrow Y_j$. If $V_{lj'} \neq 0$ for some $j' \neq j$, then Y_j must be an ancestor of $Y_{j'}$, which contradicts the fact that Y_j is a leaf node variable.

Conversely, suppose that $V_{lj} \neq 0$ and $V_{lj'} = 0$ for $j' \neq j$. If Y_j is not a leaf node variable, then there exists a variable $Y_{j'}$ such that $Y_j \rightarrow Y_{j'}$ with $h_G(j) = h_G(j') + 1$, that is $U_{jj'} \neq 0$ and $(\mathbf{U}^r)_{jj'} = 0$ for $r > 1$. Then $V_{lj'} = W_{lj} U_{jj'} \neq 0$, a contradiction.

B.3 Proof of Proposition 3

Suppose $Y_k \rightarrow Y_j$ and $h_G(j) = h_G(k) - 1$. Let X_l be an instrument of Y_k in G' . Then there are two cases: (1) X_l intervenes on Y_k but does not intervene on Y_j , namely $X_l \rightarrow Y_k$ but $X_l \not\rightarrow Y_j$; (2) X_l intervenes on Y_k and Y_j simultaneously, namely $X_l \rightarrow Y_k$ and $X_l \rightarrow Y_j$. For (1), $V_{lj} = W_{lk} U_{kj} \neq 0$. For (2), Assumption 1B implies that $V_{lj} \neq 0$. This holds for every instrument of Y_k in G' , and the desired result follows.

Conversely, suppose for each instrument X_l of Y_k in G' , we have $V_{lj} \neq 0$. Let $X_{l'}$ be an instrument of Y_k in G , which is also an instrument in G' . Then $0 \neq V_{l'j} = W_{l'k} U_{kj}$, which implies $U_{kj} \neq 0$. This completes the proof.

B.4 Proof of Theorem 4

The proof proceeds in two steps: (A) Show that $\{l : \widehat{V}_{lj} \neq 0\} = \{l : V_{lj}^\circ \neq 0\}$ almost surely for $j = 1, \dots, p$; and (B) Show that $\widehat{S} = S^\circ$ if $\widehat{\mathbf{V}}$ satisfies the property in (A). As a result, $\widehat{\mathcal{D}} = \mathcal{D}^\circ$ follows immediately.

PROOF OF (A)

Let $A_j^\circ = \{l : V_{lj}^\circ \neq 0\}$ and $A_j^{[t]} = \{l : |\widehat{V}_{lj}^{[t]}| \geq \tau_j\}$ be the estimated support of penalized solution at the t -th iteration of Algorithm 1. For the penalized solution, define the false negative set $\text{FN}_j^{[t]} = A_j^\circ \setminus A_j^{[t]}$ and the false positive set $\text{FP}_j^{[t]} = A_j^{[t]} \setminus A_j^\circ$; $t \geq 0$. Consider a “good” event $\mathcal{E}_j = \{\|\mathbf{X}^\top \widehat{\boldsymbol{\xi}}_j/n\|_\infty \leq 0.5\gamma_j\tau_j\} \cap \{\|\widehat{\mathbf{V}}_{\cdot j}^\circ - \mathbf{V}_{\cdot j}^\circ\|_\infty \leq 0.5\tau_j\}$, where $\widehat{\boldsymbol{\xi}}_j = \mathbf{Y}_j - \mathbf{X}\widehat{\mathbf{V}}_{\cdot j}^\circ$ is the residual of the least squares estimate $\widehat{\mathbf{V}}_{\cdot j}^\circ$ such that $A_j^\circ = \{l : \widehat{V}_{lj}^\circ \neq 0\}$; $j = 1, \dots, p$. We shall show that $\text{FN}_j^{[t]}$ and $\text{FP}_j^{[t]}$ are eventually empty sets on event \mathcal{E}_j which has a probability tending to one.

First, we show that if $|A_j^\circ \cup A_j^{[t-1]}| \leq 2\kappa_{\max}^\circ$ on \mathcal{E}_j for $t \geq 1$, then $|A_j^\circ \cup A_j^{[t]}| \leq 2\kappa_{\max}^\circ$, to be used in Assumption 2. Now suppose $|A_j^\circ \cup A_j^{[t-1]}| \leq 2\kappa_{\max}^\circ$ on \mathcal{E}_j for $t \geq 1$. By the optimality condition of (8),

$$\left(\widehat{\mathbf{V}}_{\cdot j}^\circ - \widetilde{\mathbf{V}}_{\cdot j}^{[t]}\right)^\top \left(-\mathbf{X}^\top (\mathbf{Y}_j - \mathbf{X}\widetilde{\mathbf{V}}_{\cdot j}^{[t]})/n + \gamma_j\tau_j \nabla \|\widetilde{\mathbf{V}}_{(A_j^{[t-1])c,j}^{[t]}}\|_1\right) \geq 0,$$

where $\widetilde{\mathbf{V}}^{[t]}$ is defined in (8). Plugging $\widehat{\boldsymbol{\xi}}_j = \mathbf{Y}_j - \mathbf{X}\widehat{\mathbf{V}}_{\cdot j}^\circ$ into the inequality and rearranging it, we have $\|\mathbf{X}(\widetilde{\mathbf{V}}_{\cdot j}^{[t]} - \widehat{\mathbf{V}}_{\cdot j}^\circ)\|_2^2/n$ is no greater than

$$\begin{aligned} & \left(\widetilde{\mathbf{V}}_{\cdot j}^{[t]} - \widehat{\mathbf{V}}_{\cdot j}^\circ\right)^\top \left(\mathbf{X}^\top \widehat{\boldsymbol{\xi}}_j/n - \gamma_j\tau_j \nabla \|\widetilde{\mathbf{V}}_{(A_j^{[t-1])c,j}^{[t]}}\|_1\right) \\ &= \left(\widetilde{\mathbf{V}}_{A_j^\circ \setminus A_j^{[t-1],j}^{[t]}} - \widehat{\mathbf{V}}_{A_j^\circ \setminus A_j^{[t-1],j}^\circ}\right)^\top \left(\mathbf{X}_{A_j^\circ \setminus A_j^{[t-1],j}^{[t]}}^\top \widehat{\boldsymbol{\xi}}_j/n - \gamma_j\tau_j \nabla \|\widetilde{\mathbf{V}}_{A_j^\circ \setminus A_j^{[t-1],j}^{[t]}}\|_1\right) \\ & \quad + \left(\widetilde{\mathbf{V}}_{(A_j^\circ \cup A_j^{[t-1])c,j}^{[t]}} - \widehat{\mathbf{V}}_{(A_j^\circ \cup A_j^{[t-1])c,j}^\circ}\right)^\top \left(\mathbf{X}^\top \widehat{\boldsymbol{\xi}}_j/n - \gamma_j\tau_j \nabla \|\widetilde{\mathbf{V}}_{(A_j^\circ \cup A_j^{[t-1])c,j}^{[t]}}\|_1\right) \\ & \quad + \left(\widetilde{\mathbf{V}}_{A_j^{[t-1]} \setminus A_j^\circ,j} - \widehat{\mathbf{V}}_{A_j^{[t-1]} \setminus A_j^\circ,j}^\circ\right)^\top \mathbf{X}_{A_j^{[t-1]} \setminus A_j^\circ,j}^\top \widehat{\boldsymbol{\xi}}_j/n. \end{aligned} \tag{29}$$

Note that

$$\left(\widetilde{\mathbf{V}}_{(A_j^\circ \cup A_j^{[t-1])c,j}^{[t]}} - \widehat{\mathbf{V}}_{(A_j^\circ \cup A_j^{[t-1])c,j}^\circ}\right)^\top \nabla \|\widetilde{\mathbf{V}}_{(A_j^\circ \cup A_j^{[t-1])c,j}^{[t]}}\|_1 = \left\| \widetilde{\mathbf{V}}_{(A_j^\circ \cup A_j^{[t-1])c,j}^{[t]}} - \widehat{\mathbf{V}}_{(A_j^\circ \cup A_j^{[t-1])c,j}^\circ} \right\|_1.$$

Then (29) is no greater than

$$\begin{aligned} & \left\| \widetilde{\mathbf{V}}_{A_j^\circ \Delta A_j^{[t-1],j}^{[t]}} - \widehat{\mathbf{V}}_{A_j^\circ \Delta A_j^{[t-1],j}^\circ} \right\|_1 \left(\|\mathbf{X}^\top \widehat{\boldsymbol{\xi}}_j/n\|_\infty + \gamma_j\tau_j \right) \\ & \quad + \left\| \widetilde{\mathbf{V}}_{(A_j^\circ \cup A_j^{[t-1])c,j}^{[t]}} - \widehat{\mathbf{V}}_{(A_j^\circ \cup A_j^{[t-1])c,j}^\circ} \right\|_1 \left(\|\mathbf{X}^\top \widehat{\boldsymbol{\xi}}_j/n\|_\infty - \gamma_j\tau_j \right), \end{aligned} \tag{30}$$

where Δ denotes the symmetric difference. Note that $\|\mathbf{X}(\tilde{\mathbf{V}}_j^{[t]} - \hat{\mathbf{V}}_j^\circ)\|_2^2/n \geq 0$. Rearranging the inequality yields that

$$\begin{aligned} & \left(\gamma_j \tau_j - \|\mathbf{X}^\top \hat{\boldsymbol{\xi}}_j/n\|_\infty \right) \left\| \tilde{\mathbf{V}}_{(A_j^\circ \cup A_j^{[t-1]})^c, j}^{[t]} - \hat{\mathbf{V}}_{(A_j^\circ \cup A_j^{[t-1]})^c, j}^\circ \right\|_1 \\ & \leq \left(\|\mathbf{X}^\top \hat{\boldsymbol{\xi}}_j/n\|_\infty + \gamma_j \tau_j \right) \left\| \tilde{\mathbf{V}}_{A_j^\circ \Delta A_j^{[t-1]}, j}^{[t]} - \hat{\mathbf{V}}_{A_j^\circ \Delta A_j^{[t-1]}, j}^\circ \right\|_1. \end{aligned}$$

On event \mathcal{E}_j , $\|\mathbf{X}^\top \hat{\boldsymbol{\xi}}_j/n\|_\infty \leq \gamma_j \tau_j/2$, implying that $\left\| \tilde{\mathbf{V}}_{(A_j^\circ \cup A_j^{[t-1]})^c, j}^{[t]} - \hat{\mathbf{V}}_{(A_j^\circ \cup A_j^{[t-1]})^c, j}^\circ \right\|_1 \leq 3 \left\| \tilde{\mathbf{V}}_{A_j^\circ \Delta A_j^{[t-1]}, j}^{[t]} - \hat{\mathbf{V}}_{A_j^\circ \Delta A_j^{[t-1]}, j}^\circ \right\|_1$. Note that $|A_j^\circ \cup A_j^{[t-1]}| \leq 2\kappa_{\max}^\circ$. By Assumption 2 and (30),

$$\begin{aligned} c_1 \|\tilde{\mathbf{V}}_j^{[t]} - \hat{\mathbf{V}}_j^\circ\|_2^2 & \leq \left(\|\mathbf{X}^\top \hat{\boldsymbol{\xi}}_j/n\|_\infty + \gamma_j \tau_j \right) \left\| \tilde{\mathbf{V}}_{A_j^\circ \Delta A_j^{[t-1]}, j}^{[t]} - \hat{\mathbf{V}}_{A_j^\circ \Delta A_j^{[t-1]}, j}^\circ \right\|_1 \\ & \quad + \left(\|\mathbf{X}^\top \hat{\boldsymbol{\xi}}_j/n\|_\infty - \gamma_j \tau_j \right) \left\| \tilde{\mathbf{V}}_{(A_j^\circ \cup A_j^{[t-1]})^c, j}^{[t]} - \hat{\mathbf{V}}_{(A_j^\circ \cup A_j^{[t-1]})^c, j}^\circ \right\|_1 \quad (31) \\ & \leq \left(\|\mathbf{X}^\top \hat{\boldsymbol{\xi}}_j/n\|_\infty + \gamma_j \tau_j \right) \left\| \tilde{\mathbf{V}}_{A_j^\circ \Delta A_j^{[t-1]}, j}^{[t]} - \hat{\mathbf{V}}_{A_j^\circ \Delta A_j^{[t-1]}, j}^\circ \right\|_1. \end{aligned}$$

By the Cauchy-Schwarz inequality, $\left\| \tilde{\mathbf{V}}_{A_j^\circ \Delta A_j^{[t-1]}, j}^{[t]} - \hat{\mathbf{V}}_{A_j^\circ \Delta A_j^{[t-1]}, j}^\circ \right\|_1 \leq \sqrt{|A_j^\circ \Delta A_j^{[t-1]}|} \left\| \tilde{\mathbf{V}}_j^{[t]} - \hat{\mathbf{V}}_j^\circ \right\|_2$. Thus, $c_1 \|\tilde{\mathbf{V}}_j^{[t]} - \hat{\mathbf{V}}_j^\circ\|_2 \leq 1.5\gamma_j \tau_j \sqrt{2\kappa_{\max}^\circ}$, since $|A_j^\circ \Delta A_j^{[t-1]}| \leq |A_j^\circ \cup A_j^{[t-1]}| \leq 2\kappa_{\max}^\circ$ and $\|\mathbf{X}^\top \hat{\boldsymbol{\xi}}_j/n\|_\infty \leq 0.5\gamma_j \tau_j$. By the condition (1) of Theorem 4, $\gamma_j \leq c_1/6$ and $\|\tilde{\mathbf{V}}_j^{[t]} - \hat{\mathbf{V}}_j^\circ\|_2/\tau_j \leq \sqrt{\kappa_{\max}^\circ}$. On the other hand, for any $l \in \text{FP}_j^{[t]} = A_j^{[t]} \setminus A_j^\circ$, we have $|\tilde{V}_{lj}^{[t]} - \hat{V}_{lj}^\circ| = |\tilde{V}_{lj}^{[t]}| > \tau_j$. Thus, $\sqrt{|\text{FP}_j^{[t]}|} \leq \|\tilde{\mathbf{V}}_j^{[t]} - \hat{\mathbf{V}}_j^\circ\|_2/\tau_j \leq \sqrt{\kappa_{\max}^\circ}$. Consequently, $|A_j^\circ \cup A_j^{[t]}| = |A_j^\circ| + |\text{FP}_j^{[t]}| \leq 2\kappa_{\max}^\circ$ on \mathcal{E}_j for $t \geq 1$.

Next, we estimate the number of iterations required for termination. Note that the machine precision is negligible. The termination criterion is met when $A_j^{[t]} = A_j^{[t-1]}$ since the weighted Lasso problem (8) remains same at the t th and $(t-1)$ th iterations. To show that $A_j^{[t]} = A_j^\circ$ eventually, we prove that $|\text{FN}_j^{[t]}| + |\text{FP}_j^{[t]}| < 1$ eventually.

Now, suppose $|\text{FN}_j^{[t]}| + |\text{FP}_j^{[t]}| \geq 1$. For any $l \in \text{FN}_j^{[t]} \cup \text{FP}_j^{[t]}$, by Assumption 4, $|\tilde{V}_{lj}^{[t]} - \hat{V}_{lj}^\circ| \geq |\tilde{V}_{lj}^{[t]} - V_{lj}^\circ| - |\hat{V}_{lj}^\circ - V_{lj}^\circ| \geq \tau_j - 0.5\tau_j$, so $\sqrt{|\text{FN}_j^{[t]}| + |\text{FP}_j^{[t]}|} \leq \|\tilde{\mathbf{V}}_j^{[t]} - \hat{\mathbf{V}}_j^\circ\|_2/0.5\tau_j$. By (31) and the Cauchy-Schwarz inequality, $c_1 \|\tilde{\mathbf{V}}_j^{[t]} - \hat{\mathbf{V}}_j^\circ\|_2 \leq 1.5\gamma_j \tau_j \sqrt{|\text{FN}_j^{[t-1]}| + |\text{FP}_j^{[t-1]}|}$. By conditions (1) and (2) for (τ_j, γ_j) in Theorem 4, we have

$$\begin{aligned} \sqrt{|\text{FN}_j^{[t]}| + |\text{FP}_j^{[t]}|} & \leq \frac{\|\tilde{\mathbf{V}}_j^{[t]} - \hat{\mathbf{V}}_j^\circ\|_2}{0.5\tau_j} \leq \frac{3\gamma_j}{c_1} \sqrt{|\text{FN}_j^{[t-1]}| + |\text{FP}_j^{[t-1]}|} \\ & \leq 0.5 \sqrt{|\text{FN}_j^{[t-1]}| + |\text{FP}_j^{[t-1]}|}. \end{aligned}$$

Hence, $\sqrt{|\text{FN}_j^{[t]}| + |\text{FP}_j^{[t]}|} \leq (1/2)^t \sqrt{|A_j^\circ| + |A_j^{[0]}|}$. In particular, for $t \geq 1 + \lceil \log \kappa_j^\circ / \log 4 \rceil$, $|\text{FN}_j^{[t]}| + |\text{FP}_j^{[t]}| < 1$ implying that $\text{FN}_j^{[t]} = \emptyset$ and $\text{FP}_j^{[t]} = \emptyset$.

Let $t_{\max} = 1 + \lceil \log \kappa_j^\circ / \log 4 \rceil$. Then $\text{FN}_j^{[t_{\max}]} = \text{FP}_j^{[t_{\max}]} = \emptyset$ on event \mathcal{E}_j . Under condition (3), we have $\{l : \tilde{V}_{lj}^{[t_{\max}]} \neq 0\} = \{l : V_{lj}^\circ \neq 0\}$. To bound $\mathbb{P}(\bigcup_{j=1}^p \mathcal{E}_j^c)$, let $\boldsymbol{\eta} = \mathbf{X}^\top (\mathbf{I} - \mathbf{P}_{A_j^\circ}) \boldsymbol{\xi}_j$ and $\boldsymbol{\eta}' = n(\mathbf{X}_{A_j^\circ}^\top \mathbf{X}_{A_j^\circ})^{-1} \mathbf{X}_{A_j^\circ}^\top \boldsymbol{\xi}_j$, where $\boldsymbol{\xi}_j = ((\varepsilon_V)_{1j}, \dots, (\varepsilon_V)_{nj})^\top \in \mathbb{R}^n$. Then $\boldsymbol{\eta} \in \mathbb{R}^q$ and $\boldsymbol{\eta}' \in \mathbb{R}^{|\kappa_j^\circ|}$ are Gaussian random vectors, where $\text{Var}(\boldsymbol{\eta}) \leq \Omega_{jj}^{-1} (\mathbf{X}^\top \mathbf{X})_{ll} \leq n\Omega_{jj}^{-1} c_2^2$ and $\text{Var}(\boldsymbol{\eta}') \leq \Omega_{jj}^{-1} ((\mathbf{X}_{A_j^\circ}^\top \mathbf{X}_{A_j^\circ})^{-1})_{ll} \leq n\Omega_{jj}^{-1} c_2^2$. Then

$$\begin{aligned} \mathbb{P}\left(\|\mathbf{X}^\top \widehat{\boldsymbol{\xi}}_j / n\|_\infty > 0.5\gamma_j\tau_j\right) &= \mathbb{P}\left(\|\boldsymbol{\eta} / n\|_\infty > 0.5\gamma_j\tau_j\right) \\ &\leq \sum_{l=1}^q \mathbb{P}\left(|\eta_l| \geq 0.5n\gamma_j\tau_j\right) \\ &\leq q \int_{\frac{0.5\sqrt{n\Omega_{jj}\gamma_j\tau_j}}{c_2}}^\infty \frac{e^{-t^2/2}}{\sqrt{2\pi}} dt \leq q\sqrt{\frac{2}{\pi}} \exp\left(-\frac{n\Omega_{jj}\gamma_j^2\tau_j^2}{8c_2^2}\right), \end{aligned}$$

and similarly,

$$\mathbb{P}\left(\|\widehat{\mathbf{V}}_{\cdot j}^\circ - \mathbf{V}_{\cdot j}^\circ\|_\infty > 0.5\tau_j\right) \leq \sum_{l \in A_j^\circ} \mathbb{P}\left(|\eta'_l| > 0.5\tau_j\right) \leq \kappa_{\max}^\circ \sqrt{\frac{2}{\pi}} \exp\left(-\frac{n\Omega_{jj}\tau_j^2}{8c_2^2}\right).$$

Under conditions (1) and (2) for (τ_j, γ_j) in Theorem 4,

$$\begin{aligned} &\mathbb{P}\left(\left\{l : \tilde{V}_{lj}^{[t_{\max}]} \neq 0\right\} = \left\{l : V_{lj}^\circ \neq 0\right\}; 1 \leq j \leq p\right) \\ &\geq 1 - \mathbb{P}\left(\bigcup_{j=1}^p \mathcal{E}_j^c\right) \\ &\geq 1 - p\sqrt{\frac{2}{\pi}} \left(e^{-4(\log(q)+\log(n))+\log(q)} + e^{-144c_1^{-2}c_2^2(\log(q)+\log(n))+\log(\kappa_j^\circ)}\right) \geq 1 - \sqrt{\frac{2}{\pi}} pq^{-3}n^{-4}. \end{aligned}$$

By Borel-Cantelli lemma, $\{l : \tilde{V}_{lj}^{[t_{\max}]} \neq 0\} = \{l : V_{lj}^\circ \neq 0\}; j = 1, \dots, p$ almost surely as $n \rightarrow \infty$.

So far, we have $\tilde{\mathbf{V}}_{\cdot j} = \tilde{\mathbf{V}}_{\cdot j}^{[t_{\max}]} = \widehat{\mathbf{V}}_{\cdot j}^\circ; j = 1, \dots, p$, almost surely. It remains to show that $\widehat{\mathbf{V}}_{\cdot j}^\circ$ is a global minimizer of (7); $j = 1, \dots, p$, with a high probability. Note that Assumptions 2 and 4 imply the degree of separation condition (Shen et al., 2013). By Theorem 2 of Shen et al. (2013),

$$\mathbb{P}\left(\widehat{\mathbf{V}}_{\cdot j}^\circ \text{ is not a global minimizer of (7); } 1 \leq j \leq p\right) \leq 3p \exp\left(-2(\log(q) + \log(n))\right).$$

implying that $\widehat{\mathbf{V}}_{\cdot j} = \tilde{\mathbf{V}}_{\cdot j}^{[t_{\max}]} = \widehat{\mathbf{V}}_{\cdot j}^\circ$ is a global minimizer of (7) almost surely, as $n \rightarrow \infty$. This completes the proof.

PROOF OF (B)

Assume $\widehat{\mathbf{V}}$ satisfies the properties in (A). Then Propositions 2 and 3 holds true for $\widehat{\mathbf{V}}$. Clearly, we have $\widehat{\mathcal{C}} = \mathcal{C}^\circ$. Thus, we need to show $\widehat{\mathcal{A}} = \mathcal{A}^\circ$ and $\widehat{\mathcal{D}} = \mathcal{D}^\circ$. We shall prove this by induction.

For $h \geq 0$, the set of instruments on leaves in the graph $G^{[h]}$ (with primary variables $\mathbf{Y}_{\{j:h_G(j) \geq h\}}$ and intervention variables \mathbf{X}) is

$$\mathcal{I}^{[h]} = \left\{ l : l = \arg \min_{l': \|\widehat{\mathbf{V}}_{l'}^{[h]}\|_0 \neq 0} \|\widehat{\mathbf{V}}_{l'}^{[h]}\|_0 \right\} = \left\{ l : \|\mathbf{V}_l^{[h]}\|_0 = 1 \right\}.$$

Hence, X_l is an instrument of leaf variable Y_j in $G^{[h]}$, when $l \in \mathcal{I}^{[h]}$ and $j = \arg \max_{j'} |V_{lj'}|$. Moreover, $h_G(j) = h$. By Proposition 3 it also recovers the edges $Y_k \rightarrow Y_j$ such that $h_G(k) = h_G(j) + 1$. In model (1), after removing $\{Y_j : h_G(j) \leq h\}$, the local Markov property among $(\mathbf{Y}_{\{j:h_G(j) \geq h+1\}}, \mathbf{X})$ remain intact provided that $\{j : h_G(j) \geq h+1\} \neq \emptyset$. Then we increment h and repeat the procedure until all primary variables are removed, namely, $\{j : h_G(j) \geq h+1\} = \emptyset$.

As a result, Algorithm 2 correctly identifies the topological height $h_G(j)$ for each primary variable Y_j and the edges $Y_k \rightarrow Y_j$ such that $h_G(k) = h_G(j) + 1$. Consequently, the ancestral relations can be reconstructed by

$$\mathcal{A} = \left\{ (k_0, k_d) : Y_{k_0} \rightarrow \cdots \rightarrow Y_{k_d}, h_G(k_\nu) = h_G(k_{\nu+1}) + 1, \nu = 0, \dots, d-1 \right\}.$$

Therefore, Step 6 of Algorithm 2 recovers $\widehat{\mathcal{A}} = \mathcal{A}^\circ$ and $\widehat{\mathcal{D}} = \mathcal{D}^\circ$ almost surely as $n \rightarrow \infty$. This completes the proof of (B).

Lemma 10 *Let*

$$T_j = \frac{\mathbf{e}_j^\top (\mathbf{P}_{A_j^\circ} - \mathbf{P}_{B_j^\circ}) \mathbf{e}_j}{\mathbf{e}_j^\top (\mathbf{I} - \mathbf{P}_{A_j^\circ}) \mathbf{e}_j / (n - |A_j^\circ|)}, \quad T_j^* = \frac{(\mathbf{e}_j^*)^\top (\mathbf{P}_{A_j^\circ} - \mathbf{P}_{B_j^\circ}) \mathbf{e}_j^*}{(\mathbf{e}_j^*)^\top (\mathbf{I} - \mathbf{P}_{A_j^\circ}) \mathbf{e}_j^* / (n - |A_j^\circ|)}, \quad (32)$$

where $A_j^\circ = \text{AN}_{S^\circ}(j) \cup \text{IN}_{S^\circ}(j) \cup \text{D}_{S^\circ}(j)$, $B_j^\circ = (\text{AN}_{S^\circ}(j) \cup \text{IN}_{S^\circ}(j)) \setminus \text{D}_{S^\circ}(j)$. Then (T_1, \dots, T_p) are independent and (T_1^*, \dots, T_p^*) are conditionally independent given \mathbf{Z} . Moreover,

$$T_j^* / (|A_j^\circ| - |B_j^\circ|) \mid \mathbf{Z} \stackrel{d}{=} T_j / (|A_j^\circ| - |B_j^\circ|) \sim F_{|A_j^\circ| - |B_j^\circ|, n - |A_j^\circ|}; \quad 1 \leq j \leq p,$$

where F_{d_1, d_2} denotes the F -distribution with d_1 and d_2 degrees of freedom.

Proof of Lemma 10

Let $\mathbf{Z} = (\mathbf{Y}, \mathbf{X})$ as in (12). Given data submatrix $\mathbf{Z}_{A_j^\circ}$,

$$\frac{\mathbf{e}_j^\top (\mathbf{P}_{A_j^\circ} - \mathbf{P}_{B_j^\circ}) \mathbf{e}_j}{\sigma_j^2} \mid \mathbf{Z}_{A_j^\circ} \sim \chi_{|A_j^\circ| - |B_j^\circ|}^2, \quad \frac{\mathbf{e}_j^\top (\mathbf{I} - \mathbf{P}_{A_j^\circ}) \mathbf{e}_j}{\sigma_j^2} \mid \mathbf{Z}_{A_j^\circ} \sim \chi_{n - |A_j^\circ|}^2,$$

and they are independent, because $\mathbf{P}_{A_j^\circ} - \mathbf{P}_{B_j^\circ}$ and $\mathbf{I} - \mathbf{P}_{A_j^\circ}$ are orthonormal projection matrices, $\mathbf{e}_j \mid \mathbf{Z}_{A_j^\circ} \sim N(\mathbf{0}, \sigma_j^2 \mathbf{I}_n)$, and $(\mathbf{P}_{A_j^\circ} - \mathbf{P}_{B_j^\circ})(\mathbf{I} - \mathbf{P}_{A_j^\circ}) = \mathbf{0}$. Then, for any $t \in \mathbb{R}$, the characteristic function $\mathbb{E} \exp(itT_j / (|A_j^\circ| - |B_j^\circ|))$ can be written as (i is the imaginary unit)

$$\mathbb{E} \left(\mathbb{E} \left(\exp(itT_j / (|A_j^\circ| - |B_j^\circ|)) \mid \mathbf{Z}_{A_j^\circ} \right) \right) = \mathbb{E} \psi_{|A_j^\circ| - |B_j^\circ|, n - |A_j^\circ|}(t) = \psi_{|A_j^\circ| - |B_j^\circ|, n - |A_j^\circ|}(t),$$

where $\psi_{|A_j^\circ| - |B_j^\circ|, n - |A_j^\circ|}$ is the characteristic function of F-distribution with degrees of freedom $|A_j^\circ| - |B_j^\circ|, n - |A_j^\circ|$. Hence, $T_j / (|A_j^\circ| - |B_j^\circ|) \sim F_{|A_j^\circ| - |B_j^\circ|, n - |A_j^\circ|}$. Similarly, $T_j^* / (|A_j^\circ| - |B_j^\circ|) \sim F_{|A_j^\circ| - |B_j^\circ|, n - |A_j^\circ|}$; $j = 1, \dots, p$.

Next, we prove independence for \mathbf{T} and \mathbf{T}^* via a peeling argument. Let $\mathbf{t} = (t_1, \dots, t_p)$. Let j be a leaf node of the graph G° . Then $\mathbf{T}_{-j} \mid \mathbf{Y}_{-j}, \mathbf{X}$ is deterministic, where \mathbf{T}_{-j} is the subvector of \mathbf{T} with the j th component removed. The characteristic function of $\mathbf{t}^\top \mathbf{T}$ is

$$\begin{aligned} \mathbb{E} \exp(\mathbf{t}^\top \mathbf{T}) &= \mathbb{E} \left(\mathbb{E} \left(\exp(\mathbf{t}^\top \mathbf{T}) \mid \mathbf{Y}_{-j}, \mathbf{X} \right) \exp(\mathbf{t}^\top \mathbf{T}_{-j}) \right) \\ &= \psi_{|A_j^\circ| - |B_j^\circ|, n - |A_j^\circ|}(t_j) \mathbb{E} \exp(\mathbf{t}^\top \mathbf{T}_{-j}), \end{aligned} \quad (33)$$

where $\psi_{|A_j^\circ| - |B_j^\circ|, n - |A_j^\circ|}$ is the characteristic function of the F-distribution with degrees of freedom $(|A_j^\circ| - |B_j^\circ|, n - |A_j^\circ|)$. Next, let j' be a leaf node of the graph G' and apply the law of iterated expectation again, where G' is the subgraph of G° without node j . Repeat this procedure and after p steps $\mathbb{E} \exp(\mathbf{t}^\top \mathbf{T}) = \prod_{j=1}^p \psi_{|A_j^\circ| - |B_j^\circ|, n - |A_j^\circ|}(t_j)$, which implies (T_1, \dots, T_p) are independent. Similarly, \mathbf{T}^* also has independent components given \mathbf{Z} and has the same distribution as \mathbf{T} . This completes the proof.

B.5 Proof of Theorem 5

PROOF OF (A)

Without loss of generality, assume M is sufficiently large. For any $x \in \mathbb{R}$,

$$\begin{aligned} &|\mathbb{P}(\text{Lr} \leq x) - \mathbb{P}(\text{Lr}(S^\circ, \widehat{\Sigma}) \leq x)| \\ &\leq \mathbb{E} |\text{I}(\text{Lr} \leq x) - \text{I}(\text{Lr}(S^\circ, \widehat{\Sigma}) \leq x)| \\ &= \mathbb{E} |\text{I}(\text{Lr} \leq x, \widehat{S} \neq S^\circ) + \text{I}(\text{Lr}(S^\circ, \widehat{\Sigma}) \leq x)(\text{I}(\widehat{S} = S^\circ) - 1)| \\ &\leq 2\mathbb{P}(\widehat{S} \neq S^\circ). \end{aligned} \quad (34)$$

From (13), $\text{Lr}^*(S^\circ, \widehat{\Sigma}^*) = \sum_{j: \text{D}_{S^\circ}(j) \neq \emptyset} T_j^*$. By Lemma 10, $\mathbb{P}(\text{Lr}(S^\circ, \widehat{\Sigma}) \leq x) = \mathbb{P}(\text{Lr}^*(S^\circ, \widehat{\Sigma}^*) \leq x \mid \mathbf{Z})$. Note that $\text{Lr}^* = \text{Lr}^*(\widehat{S}^*, \widehat{\Sigma}^*)$. Then for any $x \in \mathbb{R}$,

$$\begin{aligned} &|\mathbb{P}(\text{Lr}^* \leq x \mid \mathbf{Z}) - \mathbb{P}(\text{Lr}(S^\circ, \widehat{\Sigma}) \leq x)| \\ &= |\mathbb{P}(\text{Lr}^* \leq x, \widehat{S}^* \neq S^\circ \mid \mathbf{Z}) + \mathbb{P}(\text{Lr}^* \leq x, \widehat{S}^* = S^\circ \mid \mathbf{Z}) - \mathbb{P}(\text{Lr}^*(S^\circ, \widehat{\Sigma}^*) \leq x \mid \mathbf{Z})| \\ &\leq |\mathbb{P}(\text{Lr}^* \leq x, \widehat{S}^* \neq S^\circ \mid \mathbf{Z})| + |\mathbb{P}(\text{Lr}^*(S^\circ, \widehat{\Sigma}^*) \leq x, \widehat{S}^* \neq S^\circ \mid \mathbf{Z})| \\ &\leq 2\mathbb{P}(\widehat{S}^* \neq S^\circ \mid \mathbf{Z}). \end{aligned} \quad (35)$$

Since (34) and (35) hold uniformly in x , we have

$$\sup_{x \in \mathbb{R}} |\mathbb{P}(\text{Lr} \leq x) - \mathbb{P}(\text{Lr}^* \leq x \mid \mathbf{Z})| \leq 2\mathbb{P}(\widehat{S} \neq S^\circ) + 2\mathbb{P}(\widehat{S}^* \neq S^\circ \mid \mathbf{Z}).$$

By Theorem 4, we have $\mathbb{P}(\widehat{S} \neq S^\circ) \rightarrow 0$, which holds uniformly for all $\boldsymbol{\theta}$ which satisfy the Assumptions 1C-5. For $\mathbb{P}(\widehat{S}^* \neq S^\circ \mid \mathbf{Z})$, the error terms of (7) in the perturbed data \mathbf{Z}^* are rescaled with $\Omega_{jj}^{-1} + \widehat{\sigma}_j^2 \leq 2\Omega_{jj}^{-1}$. By Theorem 4, $\mathbb{P}(\widehat{S}^* \neq S^\circ) = \mathbb{E} \mathbb{P}(\widehat{S}^* \neq S^\circ \mid \mathbf{Z}) \rightarrow 0$,

which implies $\mathbb{P}(\widehat{S}^* \neq S^\circ \mid \mathbf{Z}) \xrightarrow{p} 0$ as $n \rightarrow \infty$ by the Markov inequality. Consequently, $\sup_{x \in \mathbb{R}} |\mathbb{P}(\text{Lr} \leq x) - \mathbb{P}(\text{Lr}^* \leq x \mid \mathbf{Z})| \rightarrow 0$. For $|\mathcal{D}| = 0$, $\mathbb{P}(\text{Lr} = 0) \rightarrow 1$, $\mathbb{P}(\text{Lr}^* = 0 \mid \mathbf{Z}) \rightarrow 1$, and $\mathbb{P}(\text{Pval} = 1) \rightarrow 1$. For $|\mathcal{D}| > 0$, $\mathbb{P}(\text{Lr}^* \geq \text{Lr} \mid \mathbf{Z}) \rightarrow \text{Unif}(0, 1)$ and $\mathbb{P}(\text{Pval} < \alpha) \rightarrow \alpha$. This completes the proof of (A).

PROOF OF (B)

Let $\text{Pval}_k = M^{-1} \sum_{m=1}^M \mathbf{I}(\text{Lr}_{k,m}^* \geq \text{Lr})$, the p-value of sub-hypothesis $H_{0,k}$. For $|\mathcal{D}| < |\mathcal{H}|$, there exists an edge $(i_k, j_k) \in \mathcal{H}$ but $(i_k, j_k) \notin \mathcal{D}$. Then by (A), $\mathbb{P}(\text{Pval} = \text{Pval}_k = 1) \rightarrow 1$. For $|\mathcal{D}| = |\mathcal{H}|$, note that as $n, M \rightarrow \infty$,

$$\mathbb{P}(\text{Pval} < \alpha) = \mathbb{P}(\text{Pval}_1 < \alpha, \dots, \text{Pval}_{|\mathcal{H}|} < \alpha) \leq \mathbb{P}(\text{Pval}_1 < \alpha) \rightarrow \alpha.$$

Now, define a sequence $\mathbf{U}_{\mathcal{H}}^{(r)}$; $r = 1, 2, \dots$ such that $\mathbf{U}_{(i_1, j_1)}^{(r)} = 0$ and $\min_{k=2}^{|\mathcal{H}|} |\mathbf{U}_{(i_k, j_k)}^{(r)}| \geq c > 0$. Thus, $\mathbf{U}_{\mathcal{H}}^{(r)}$; $r = 1, 2, \dots$ satisfies H_0 . By Proposition 7, $\text{Pval}_k \xrightarrow{p} 0$ for $k \geq 2$ as $r \rightarrow \infty$. Hence,

$$\limsup_{n \rightarrow \infty} \mathbb{P}_{\boldsymbol{\theta}^{(r)}}(\text{Pval} < \alpha) \geq \sup_r \lim_{n, p, q \rightarrow \infty} \mathbb{P}_{\boldsymbol{\theta}^{(r)}}(\text{Pval} < \alpha) = \alpha.$$

$\mathbf{U}_{\mathcal{H}}^{(r)}$ satisfies H_0

This completes the proof.

B.6 Proof of Proposition 6

Since $\mathbb{P}(\widehat{S} = S^\circ) \rightarrow 1$, it suffices to consider $\text{Lr}(S^\circ, \widehat{\boldsymbol{\Sigma}})$. For $|\mathcal{D}| = 0$, we have $\mathbb{P}(\text{Lr} = 0) \rightarrow 1$. Now, assume $|\mathcal{D}| > 0$. Then

$$2\text{Lr}(S^\circ, \widehat{\boldsymbol{\Sigma}}) = \underbrace{\sum_{j: \mathcal{D}_{S^\circ}(j) \neq \emptyset} \frac{\mathbf{e}_j^\top (\mathbf{P}_{A_j^\circ} - \mathbf{P}_{B_j^\circ}) \mathbf{e}_j}{\sigma_j^2}}_{R_1} + \underbrace{\sum_{j: \mathcal{D}_{S^\circ}(j) \neq \emptyset} \left(\frac{\sigma_j^2}{\widehat{\sigma}_j^2} - 1 \right) \frac{\mathbf{e}_j^\top (\mathbf{P}_{A_j^\circ} - \mathbf{P}_{B_j^\circ}) \mathbf{e}_j}{\sigma_j^2}}_{R_2}.$$

To derive the asymptotic distribution of R_1 , we apply the peeling strategy with law of iterated expectation as in the proof of Lemma 10. Then we have $\mathbf{e}_j^\top (\mathbf{P}_{A_j^\circ} - \mathbf{P}_{B_j^\circ}) \mathbf{e}_j / \sigma_j^2$; $\mathcal{D}_{S^\circ}(j) \neq \emptyset$ are independent. Therefore, $R_1 \sim \chi_{|\mathcal{D}|}^2$.

To bound R_2 , we apply Lemma 1 of Laurent and Massart (2000). By Assumption 5,

$$\mathbb{P} \left(\max_{j: \mathcal{D}_{S^\circ}(j) \neq \emptyset} \left| \frac{\widehat{\sigma}_j^2}{\sigma_j^2} - 1 \right| \geq 4 \sqrt{\frac{\log |\mathcal{D}|}{(1-\rho)n}} + 8 \frac{\log |\mathcal{D}|}{(1-\rho)n} \right) \leq 2 \exp(-\log |\mathcal{D}|).$$

Hence, $\max_{j: \mathcal{D}_{S^\circ}(j) \neq \emptyset} \left| \frac{\sigma_j^2}{\widehat{\sigma}_j^2} - 1 \right| \leq 8 \sqrt{\frac{\log |\mathcal{D}|}{(1-\rho)n}}$ with probability tending one as $n, p \rightarrow \infty$. Thus

$$|R_2| \leq |R_1| \max_{j: \mathcal{D}_{S^\circ}(j) \neq \emptyset} \left| \frac{\sigma_j^2}{\widehat{\sigma}_j^2} - 1 \right| \leq O_{\mathbb{P}} \left(|\mathcal{D}| \sqrt{\frac{\log |\mathcal{D}|}{n}} \right).$$

Consequently, as $n, p, q \rightarrow \infty$, if $|\mathcal{D}| > 0$ is fixed, then $2\text{Lr} \xrightarrow{d} \chi_{|\mathcal{D}|}^2$; if $|\mathcal{D}| \rightarrow \infty$, then $(2|\mathcal{D}|)^{-1/2}(2\text{Lr} - |\mathcal{D}|) \xrightarrow{d} N(0, 1)$. This completes the proof.

B.7 Proof of Proposition 7

Let $\boldsymbol{\theta}^{(n)} = (\mathbf{U}^\circ + \boldsymbol{\Delta}, \mathbf{W}^\circ)$. Then

$$L(\boldsymbol{\theta}^{(n)}, \boldsymbol{\Sigma}^\circ) - L(\boldsymbol{\theta}^\circ, \boldsymbol{\Sigma}^\circ) = \sum_{j: \mathcal{D}^\circ(j) \neq \emptyset} \left(\sqrt{n} \boldsymbol{\eta}_j^\top \boldsymbol{\Delta}_{\cdot j} - \frac{1}{2} \sqrt{n} \boldsymbol{\Delta}_{\cdot j} \left(n^{-1} \mathbf{Y}_{\mathcal{D}^\circ(j)}^\top \mathbf{Y}_{\mathcal{D}^\circ(j)} \right) \sqrt{n} \boldsymbol{\Delta}_{\cdot j} \right),$$

where $\boldsymbol{\eta}_j = (n^{-1/2} \mathbf{Y}_{\mathcal{D}^\circ(j)}^\top \mathbf{e}_j, \mathbf{0}_{|\mathcal{D}^\circ(j)^c|}) \in \mathbb{R}^p$. For the likelihood ratio, it suffices to consider $\text{Lr}(S^\circ, \widehat{\boldsymbol{\Sigma}})$, since $P(\widehat{S} = S^\circ) \rightarrow 1$. Under H_0 , we have $2\text{Lr} = \sum_{j: \mathcal{D}^\circ(j) \neq \emptyset} T_j$. Note that $T_j = \sum_{r=1}^{|\mathcal{D}^\circ(j)|} (\mathbf{q}_{j,r}^\top \mathbf{e}_j)^2 + o_{\mathbb{P}}(1)$ by Proposition 6, where $\mathbf{P}_{A_j^\circ} - \mathbf{P}_{B_j^\circ} = \sum_{r=1}^{|\mathcal{D}^\circ(j)|} \mathbf{q}_{j,r} \mathbf{q}_{j,r}^\top$. Let $\mathbf{Q}_j = (\mathbf{q}_{j,1}, \dots, \mathbf{q}_{j,|\mathcal{D}^\circ(j)|}) \in \mathbb{R}^{n \times |\mathcal{D}^\circ(j)|}$. Then

$$\begin{aligned} \begin{pmatrix} \mathbf{Q}_j^\top \mathbf{e}_j \\ \boldsymbol{\eta}_j \end{pmatrix} \Big| \mathbf{Y}_{\text{AN}(j)}, \mathbf{X} &\sim N \left(\mathbf{0}, \begin{pmatrix} \mathbf{I}_{|\mathcal{D}^\circ(j)|} & n^{-1/2} \mathbf{Q}_j^\top \mathbf{Y}_{\mathcal{D}^\circ(j)} \\ n^{-1/2} \mathbf{Y}_{\mathcal{D}^\circ(j)}^\top \mathbf{Q}_j & n^{-1} \mathbf{Y}_{\mathcal{D}^\circ(j)}^\top \mathbf{Y}_{\mathcal{D}^\circ(j)} \end{pmatrix} \right), \\ \mathbf{Q}_j^\top \mathbf{e}_j \mid \boldsymbol{\eta}_j, \mathbf{Y}_{\text{AN}(j)}, \mathbf{X} &\sim N \left(n^{-1/2} \mathbf{Y}_{\mathcal{D}^\circ(j)}^\top \mathbf{Q}_j \boldsymbol{\eta}_j, \mathbf{Y}_{\mathcal{D}^\circ(j)}^\top (\mathbf{I}_n - \mathbf{Q}_j \mathbf{Q}_j^\top) \mathbf{Y}_{\mathcal{D}^\circ(j)} \right). \end{aligned}$$

Next, let k be a leaf node of the graph G° . For fixed $|\mathcal{D}| > 0$, after change of measure,

$$\begin{aligned} &\beta(\boldsymbol{\theta}^\circ, \boldsymbol{\Delta}) \\ &\geq \liminf_{n \rightarrow \infty} \mathbb{E}_{\boldsymbol{\theta}^\circ} \left(\mathbb{I} \left(\sum_{j=1}^p \|\mathbf{Q}_j^\top \mathbf{e}_j\|_2^2 > \chi_{|\mathcal{D}|, 1-\alpha}^2 \right) \exp(L(\boldsymbol{\theta}^{(n)}, \boldsymbol{\Sigma}^\circ) - L(\boldsymbol{\theta}^\circ, \boldsymbol{\Sigma}^\circ)) \right) \\ &= \liminf_{n \rightarrow \infty} \mathbb{E}_{\boldsymbol{\theta}^\circ} \mathbb{E} \left(\mathbb{I} \left(\sum_{j=1}^p \|\mathbf{Q}_j^\top \mathbf{e}_j\|_2^2 > \chi_{|\mathcal{D}|, 1-\alpha}^2 \right) \exp(L(\boldsymbol{\theta}^{(n)}, \boldsymbol{\Sigma}^\circ) - L(\boldsymbol{\theta}^\circ, \boldsymbol{\Sigma}^\circ)) \Big| \mathbf{Y}_{-k}, \mathbf{X} \right) \\ &= \liminf_{n \rightarrow \infty} \mathbb{E} \left(\mathbb{P} \left(\|\mathbf{Z}_k + \mathbf{Q}_k^\top \mathbf{Y}_{\mathcal{D}^\circ(k)} \boldsymbol{\Delta}_{\cdot k}\|_2^2 + \sum_{j \neq k} \|\mathbf{Q}_j^\top \mathbf{e}_j\|_2^2 > \chi_{|\mathcal{D}|, 1-\alpha}^2 \Big| \mathbf{Y}_{-k}, \mathbf{X} \right) \right), \end{aligned}$$

where $\mathbf{Z}_k \sim N(\mathbf{0}, \mathbf{I}_{|\mathcal{D}^\circ(k)|})$. By Lemma 3 of Li et al. (2019), $\|\mathbf{Q}_k^\top \mathbf{Y}_{\mathcal{D}^\circ(k)} \boldsymbol{\Delta}_{\cdot k}\|_2^2 \geq c_3 \|\boldsymbol{\Delta}_{\cdot k}\|_2^2$ with probability tending to one. Therefore, a peeling argument yields

$$\beta(\boldsymbol{\theta}^\circ, \boldsymbol{\Delta}) \geq \mathbb{P} \left(\|\mathbf{Z} + c_3 \boldsymbol{\Delta}\|_2^2 \geq \chi_{|\mathcal{D}|, 1-\alpha}^2 \right),$$

where $\mathbf{Z} \sim N(\mathbf{0}, \mathbf{I}_{|\mathcal{D}|})$. Similarly, as $|\mathcal{D}| \rightarrow \infty$,

$$\beta(\boldsymbol{\theta}^\circ, \mathbf{H}) \geq \mathbb{P} \left(\|\mathbf{Z} + c_3 \boldsymbol{\Delta}\|_2^2 > \sqrt{2|\mathcal{D}|} z_{1-\alpha} + |\mathcal{D}| \right) \rightarrow \mathbb{P} \left(Z > z_{1-\alpha} - c_3 \|\boldsymbol{\Delta}\|_2 / \sqrt{2|\mathcal{D}|} \right).$$

This completes the proof.

B.8 Proof of Proposition 8

By Proposition 7, for fixed $|\mathcal{D}| = |\mathcal{H}| > 0$, $\beta(\boldsymbol{\theta}^\circ, \boldsymbol{\Delta})$ equals to

$$\mathbb{P}(\text{Pval}_1 < \alpha, \dots, \text{Pval}_{|\mathcal{H}|} < \alpha) \geq 1 - \sum_{k=1}^{|\mathcal{H}|} \mathbb{P}(\text{Pval}_k \leq \alpha) \geq 1 - |\mathcal{H}| \mathbb{P}(Z_1^2 \leq \chi_{1, 1-\alpha}^2),$$

where $Z_1 \sim N(\delta/\max_{1 \leq j \leq p} \Omega_{jj}, 1)$. Then $\mathbb{P}(\tilde{Z}^2 \leq x) \leq \mathbb{P}(\tilde{Z} \leq -\mu + \sqrt{x}) \leq \frac{1}{\sqrt{2\pi}} \frac{e^{-(\mu - \sqrt{x})^2/2}}{\mu - \sqrt{x}}$ for $\tilde{Z} \sim N(\mu, 1)$ and any $0 \leq x < \mu^2$ and $\mu > 0$ (Small, 2010). Hence, as $|\mathcal{D}| = |\mathcal{H}| \rightarrow \infty$,

$$\beta(\boldsymbol{\theta}^\circ, \boldsymbol{\Delta}) \geq 1 - |\mathcal{H}| \mathbb{P}(Z_1^2 \leq \chi_{1,1-\alpha}^2) \geq 1 - \frac{|\mathcal{H}|}{\sqrt{2\pi}} e^{-\left(\delta\sqrt{\log|\mathcal{H}|}/\max_{1 \leq j \leq p} \Omega_{jj} - \sqrt{\chi_{1,1-\alpha}^2}\right)^2/2} \rightarrow 1.$$

This completes the proof.

B.9 Proof of Theorem 9

The proof proceeds in two steps to show that (A) $\{l : |V_{lj}^\circ| \geq \tau_j^*\} \subseteq \{l : \hat{V}_{lj} \neq 0\} \subseteq \{l : V_{lj}^\circ \neq 0\}$ for $1 \leq j \leq p$ almost surely and (B) $\hat{\mathcal{A}} = \mathcal{A}^\circ$ when $\hat{\mathbf{V}}$ satisfies the property in (A). Then $\hat{\mathcal{D}} = \mathcal{D}^\circ$ follows immediately.

PROOF OF (A)

This proof is similar to that of Theorem 4 part (A). Let $A_j^\circ = \{l : V_{lj}^\circ \neq 0\}$, $A_j^* = \{l : |V_{lj}^\circ| > \tau_j^*\}$, and $A_j^{[t]} = \{l : |\tilde{V}_{lj}^{[t]}| > \tau_j\}$. Define the false negative set $\text{FN}_j^{[t]} = A_j^* \setminus A_j^{[t]}$ and the false positive set $\text{FP}_j^{[t]} = A_j^{[t]} \setminus A_j^\circ$; $t \geq 0$. Consider $\mathcal{E}_j = \{\|\mathbf{X}^\top \hat{\boldsymbol{\xi}}_j/n\|_\infty \leq 0.5\gamma_j\tau_j\} \cap \{\|\hat{\mathbf{V}}_{\cdot j}^\circ - \mathbf{V}_{\cdot j}^\circ\|_\infty \leq 0.5\tau_j\}$, where $\hat{\boldsymbol{\xi}}_j = \mathbf{Y}_j - \mathbf{X}\hat{\mathbf{V}}_{\cdot j}^\circ$; $j = 1, \dots, p$. Again, we shall show that $\text{FN}_j^{[t]}$ and $\text{FP}_j^{[t]}$ are eventually empty on event \mathcal{E}_j which has a probability tending to one.

Assume $|A_j^\circ \cup A_j^{[t-1]}| \leq 2\kappa_{\max}^\circ$. Then (29), (30), and (31) remain true on \mathcal{E}_j . As a result, $|A_j^\circ \cup A_j^{[t]}| \leq 2\kappa_{\max}^\circ$ on \mathcal{E}_j for $t \geq 1$.

To estimate the number of iterations required for termination, it suffices to prove that $|\text{FN}_j^{[t]}| + |\text{FP}_j^{[t]}| < 1$ eventually. Suppose $|\text{FN}_j^{[t]}| + |\text{FP}_j^{[t]}| \geq 1$. For any $l \in \text{FN}_j^{[t]} \cup \text{FP}_j^{[t]}$, by Assumption 6, $|\tilde{V}_{lj}^{[t]} - \hat{V}_{lj}^\circ| \geq |\tilde{V}_{lj}^{[t]} - V_{lj}^\circ| - |\hat{V}_{lj}^\circ - V_{lj}^\circ| \geq \min(\tau_j^* - \tau_j, \tau_j)$, so $\sqrt{|\text{FN}_j^{[t]}| + |\text{FP}_j^{[t]}|} \leq \|\tilde{\mathbf{V}}_{\cdot j}^{[t]} - \hat{\mathbf{V}}_{\cdot j}^\circ\|_2 / \min(\tau_j^* - \tau_j, \tau_j)$. By (31) and the Cauchy-Schwarz inequality, $c_1 \|\tilde{\mathbf{V}}_{\cdot j}^{[t]} - \hat{\mathbf{V}}_{\cdot j}^\circ\|_2 \leq 1.5\gamma_j\tau_j \sqrt{|A_j^\circ \triangle A_j^{[t-1]}|} \leq 1.5\gamma_j\tau_j \sqrt{|\text{FN}_j^{[t-1]}| + |\text{FP}_j^{[t-1]}| + (\kappa_j^\circ - \kappa_j^*)}$. By conditions (1) and (2) for (τ_j, γ_j) in Theorem 9, we have

$$\begin{aligned} \sqrt{|\text{FN}_j^{[t]}| + |\text{FP}_j^{[t]}|} &\leq \frac{\|\tilde{\mathbf{V}}_{\cdot j}^{[t]} - \hat{\mathbf{V}}_{\cdot j}^\circ\|_2}{\min(\tau_j^* - \tau_j, \tau_j)} \\ &\leq \frac{1.5\gamma_j\tau_j}{c_1 \min(\tau_j^* - \tau_j, \tau_j)} \left(\sqrt{|\text{FN}_j^{[t-1]}| + |\text{FP}_j^{[t-1]}|} + \sqrt{\kappa_j^\circ - \kappa_j^*} \right) \\ &\leq 0.5\sqrt{|\text{FN}_j^{[t-1]}| + |\text{FP}_j^{[t-1]}|} + 0.25. \end{aligned}$$

Hence, $\sqrt{|\text{FN}_j^{[t]}| + |\text{FP}_j^{[t]}|} \leq (1/2)^t \sqrt{|A_j^\circ| + |A_j^{[0]}|} + 0.5$. For $t \geq 1 + \lceil \log \kappa_j^\circ / \log 4 \rceil$, $|\text{FN}_j^{[t]}| + |\text{FP}_j^{[t]}| < 1$ implying that $\text{FN}_j^{[t]} = \emptyset$ and $\text{FP}_j^{[t]} = \emptyset$.

Under conditions (1) and (2) for (τ_j, γ_j) in Theorem 9, using the same argument in Proof of Theorem 4 we have

$$\mathbb{P}\left(\left\{l : |V_{lj}^\circ| > \tau_j^*\right\} \subseteq \left\{l : |\tilde{V}_{lj}| > \tau_j\right\} \subseteq \left\{l : V_{lj}^\circ \neq 0\right\}; 1 \leq j \leq p\right) \geq 1 - \sqrt{\frac{2}{\pi}} pq^{-3} n^{-4}.$$

By Borel-Cantelli lemma, the event $\{l : |V_{lj}^\circ| > \tau_j^*\} \subseteq \{l : |\tilde{V}_{lj}| > \tau_j\} \subseteq \{l : V_{lj}^\circ \neq 0\}$; $j = 1, \dots, p$ almost surely as $n \rightarrow \infty$. Thus, when $\kappa_j = \kappa_j^\circ \geq |\{l : \tilde{V}_{lj} > \tau_j\}|$, we have $\{l : \hat{V}_{lj} \neq 0\} = \{l : |\tilde{V}_{lj}| > \tau_j\}$; $j = 1, \dots, p$ and satisfies the desired properties. This completes the proof.

PROOF OF (B)

This is the same as the Proof of Theorem 4 part (B).

Appendix C. Implementation details

DP-LR and LR:

- For Algorithm 3, we fix the Monte Carlo sample size $M = 500$. Our limited numerical experience suggests that this choice appears adequate for our purpose.
- For Algorithms 1 and 2, we choose $\tau_j \in \{0.05, 0.1, 0.15\}$ and $\gamma_j = \exp(\gamma'_j)$ with

$$\gamma'_j \in \left\{ \log(\max_{l,j} |\mathbf{X}_l^\top \mathbf{Y}_j|), \dots, 0.05 \log(\max_{l,j} |\mathbf{X}_l^\top \mathbf{Y}_j|) \right\} \quad (100 \text{ equally spaced values}).$$

Then BIC is used to estimate tuning parameters $\kappa_j \in \{1, \dots, 30\}$; $j = 1, \dots, p$.

2SPLS (Chen et al., 2018):

- We use the R package **BigSEM** for 2SPLS. In our experiments, the λ sequence of 2SPLS (Chen et al., 2018) is set in the same way as the γ sequence of the proposed methods. We use the default settings for other parameters.

References

- T. O. Bergmann and G. Hartwigsen. Inferring causality from noninvasive brain stimulation in cognitive neuroscience. *Journal of Cognitive Neuroscience*, 33(2):195–225, 2021.
- P. J. Bickel, Y. Ritov, A. B. Tsybakov, et al. Simultaneous analysis of lasso and dantzig selector. *The Annals of Statistics*, 37(4):1705–1732, 2009.
- L. Breiman. The little bootstrap and other methods for dimensionality selection in regression: X-fixed prediction error. *Journal of the American Statistical Association*, 87(419):738–754, 1992.
- B. C. Brown and D. A. Knowles. Phenome-scale causal network discovery with bidirectional mediated Mendelian randomization. *bioRxiv*, 2020.
- G. Bu. Apolipoprotein E and its receptors in Alzheimer’s disease: pathways, pathogenesis and therapy. *Nature Reviews Neuroscience*, 10(5):333–344, 2009.
- E. Candès, Y. Fan, L. Janson, and J. Lv. Panning for gold: ‘model-X’ knockoffs for high dimensional controlled variable selection. *Journal of the Royal Statistical Society: Series B (Statistical Methodology)*, 80(3):551–577, 2018.

- C. Chen, M. Ren, M. Zhang, and D. Zhang. A two-stage penalized least squares method for constructing large systems of structural equations. *The Journal of Machine Learning Research*, 19(1):40–73, 2018.
- D. Eaton and K. Murphy. Exact bayesian structure learning from uncertain interventions. In *Artificial Intelligence and Statistics*, pages 107–114, 2007.
- B. Efron, T. Hastie, I. Johnstone, R. Tibshirani, et al. Least angle regression. *The Annals of Statistics*, 32(2):407–499, 2004.
- J. Fan, L. Xue, H. Zou, et al. Strong oracle optimality of folded concave penalized estimation. *The Annals of Statistics*, 42(3):819–849, 2014.
- N. Friedman and D. Koller. Being Bayesian about network structure. a Bayesian approach to structure discovery in Bayesian networks. *Machine Learning*, 50(1-2):95–125, 2003.
- A. Ghoshal and J. Honorio. Learning linear structural equation models in polynomial time and sample complexity. In *International Conference on Artificial Intelligence and Statistics*, pages 1466–1475. PMLR, 2018.
- M. Grosse-Wentrup, D. Janzing, M. Siegel, and B. Schölkopf. Identification of causal relations in neuroimaging data with latent confounders: An instrumental variable approach. *NeuroImage*, 125:825–833, 2016.
- C. Heinze-Deml, M. H. Maathuis, and N. Meinshausen. Causal structure learning. *Annual Review of Statistics and Its Application*, 5:371–391, 2018.
- P. O. Hoyer, D. Janzing, J. M. Mooij, J. Peters, and B. Schölkopf. Nonlinear causal discovery with additive noise models. In *Advances in Neural Information Processing Systems*, pages 689–696, 2009.
- A. L. Jackson, S. R. Bartz, J. Schelter, S. V. Kobayashi, J. Burchard, M. Mao, B. Li, G. Cavet, and P. S. Linsley. Expression profiling reveals off-target gene regulation by rnaï. *Nature Biotechnology*, 21(6):635–637, 2003.
- J. Janková and S. van de Geer. Inference in high-dimensional graphical models. *arXiv preprint arXiv:1801.08512*, 2018.
- T. Julia and A. M. Goate. Genetics of β -amyloid precursor protein in Alzheimer’s disease. *Cold Spring Harbor Perspectives in Medicine*, 7(6):a024539, 2017.
- M. Kanehisa and S. Goto. KEGG: Kyoto encyclopedia of genes and genomes. *Nucleic Acids Research*, 28(1):27–30, 2000.
- R. J. Kelleher and J. Shen. Presenilin-1 mutations and Alzheimer’s disease. *Proceedings of the National Academy of Sciences*, 114(4):629–631, 2017.
- A. Kleiner, A. Talwalkar, P. Sarkar, and M. Jordan. The big data bootstrap. *arXiv preprint arXiv:1206.6415*, 2012.

- M. M. Kulkarni, M. Booker, S. J. Silver, A. Friedman, P. Hong, N. Perrimon, and B. Mathey-Prevot. Evidence of off-target effects associated with long dsRNAs in *Drosophila melanogaster* cell-based assays. *Nature Methods*, 3(10):833–838, 2006.
- B. Laurent and P. Massart. Adaptive estimation of a quadratic functional by model selection. *Annals of Statistics*, pages 1302–1338, 2000.
- C. Li, X. Shen, and W. Pan. Likelihood ratio tests for a large directed acyclic graph. *Journal of the American Statistical Association*, pages 1–16, 2019.
- Z. Liu, M. Zhang, G. Xu, C. Huo, Q. Tan, Z. Li, and Q. Yuan. Effective connectivity analysis of the brain network in drivers during actual driving using near-infrared spectroscopy. *Frontiers in Behavioral Neuroscience*, 11:211, 2017.
- R. Lockhart, J. Taylor, R. J. Tibshirani, and R. Tibshirani. A significance test for the Lasso. *Annals of Statistics*, 42(2):413, 2014.
- P.-L. Loh, M. J. Wainwright, et al. Support recovery without incoherence: A case for nonconvex regularization. *The Annals of Statistics*, 45(6):2455–2482, 2017.
- R. Luo and H. Zhao. Bayesian hierarchical modeling for signaling pathway inference from single cell interventional data. *The Annals of Applied Statistics*, 5(2A):725, 2011.
- T. Matsui, M. Ingelsson, H. Fukumoto, K. Ramasamy, H. Kowa, M. P. Frosch, M. C. Irizarry, and B. T. Hyman. Expression of APP pathway mRNAs and proteins in Alzheimer’s disease. *Brain Research*, 1161:116–123, 2007.
- N. Meinshausen and P. Bühlmann. Stability selection. *Journal of the Royal Statistical Society: Series B (Statistical Methodology)*, 72(4):417–473, 2010.
- A. J. Molstad, W. Sun, and L. Hsu. A covariance-enhanced approach to multitissue joint eqtl mapping with application to transcriptome-wide association studies. *The Annals of Applied Statistics*, 15(2):998–1016, 2021.
- M. P. Murray. Avoiding invalid instruments and coping with weak instruments. *Journal of economic Perspectives*, 20(4):111–132, 2006.
- C. J. Oates, J. Q. Smith, and S. Mukherjee. Estimating causal structure using conditional DAG models. *The Journal of Machine Learning Research*, 17(1):1880–1903, 2016.
- R. Pamfil, N. Sriwattanaworachai, S. Desai, P. Pilgerstorfer, K. Georgatzis, P. Beaumont, and B. Aragam. DYNOTEARS: Structure learning from time-series data. In *International Conference on Artificial Intelligence and Statistics*, pages 1595–1605. PMLR, 2020.
- J. Pearl. *Causality: Models, Reasoning and Inference*. Cambridge University Press, 2000.
- J. Peters and P. Bühlmann. Identifiability of gaussian structural equation models with equal error variances. *Biometrika*, 101(1):219–228, 2014.

- J. Peters, P. Bühlmann, and N. Meinshausen. Causal inference by using invariant prediction: identification and confidence intervals. *Journal of the Royal Statistical Society: Series B (Statistical Methodology)*, 78(5):947–1012, 2016.
- G. Rajendran, B. Kivva, M. Gao, and B. Aragam. Structure learning in polynomial time: Greedy algorithms, Bregman information, and exponential families. *Advances in Neural Information Processing Systems*, 34:18660–18672, 2021.
- P. Rolland, V. Cevher, M. Kleindessner, C. Russel, B. Schölkopf, D. Janzing, and F. Locatello. Score matching enables causal discovery of nonlinear additive noise models. *arXiv preprint arXiv:2203.04413*, 2022.
- D. Rothenhäusler, P. Bühlmann, N. Meinshausen, et al. Causal Dantzig: fast inference in linear structural equation models with hidden variables under additive interventions. *The Annals of Statistics*, 47(3):1688–1722, 2019.
- M. Rudelson and S. Zhou. Reconstruction from anisotropic random measurements. In *Conference on Learning Theory*, pages 10–1, 2012.
- K. Sachs, O. Perez, D. Pe’er, D. A. Lauffenburger, and G. P. Nolan. Causal protein-signaling networks derived from multiparameter single-cell data. *Science*, 308(5721):523–529, 2005.
- X. Shen and J. Ye. Adaptive model selection. *Journal of the American Statistical Association*, 97(457):210–221, 2002.
- X. Shen, W. Pan, and Y. Zhu. Likelihood-based selection and sharp parameter estimation. *Journal of the American Statistical Association*, 107(497):223–232, 2012.
- X. Shen, W. Pan, Y. Zhu, and H. Zhou. On constrained and regularized high-dimensional regression. *Annals of the Institute of Statistical Mathematics*, 65(5):807–832, 2013.
- S. Shimizu, P. O. Hoyer, A. Hyvärinen, and A. Kerminen. A linear non-gaussian acyclic model for causal discovery. *Journal of Machine Learning Research*, 7(Oct):2003–2030, 2006.
- A. Shojaie and G. Michailidis. Penalized likelihood methods for estimation of sparse high-dimensional directed acyclic graphs. *Biometrika*, 97(3):519–538, 2010.
- C. G. Small. *Expansions and Asymptotics for Statistics*. Chapman and Hall/CRC, 2010.
- P. Spirtes, C. Glymour, and R. Scheines. *Causation, Prediction, and Search*. The MIT Press, 2000.
- C. Squires, Y. Wang, and C. Uhler. Permutation-based causal structure learning with unknown intervention targets. In *Conference on Uncertainty in Artificial Intelligence*, pages 1039–1048. PMLR, 2020.
- J. H. Su, M. Zhao, A. J. Anderson, A. Srinivasan, and C. W. Cotman. Activated caspase-3 expression in Alzheimer’s and aged control brain: correlation with Alzheimer pathology. *Brain Research*, 898(2):350–357, 2001.

- A. Teumer. Common methods for performing Mendelian randomization. *Frontiers in Cardiovascular Medicine*, 5:51, 2018.
- C. Uhler, G. Raskutti, P. Bühlmann, and B. Yu. Geometry of the faithfulness assumption in causal inference. *The Annals of Statistics*, 41(2):436–463, 2013.
- S. van de Geer and P. Bühlmann. l_0 -penalized maximum likelihood for sparse directed acyclic graphs. *The Annals of Statistics*, 41(2):536–567, 2013.
- F. Vanleuven. GSK3 and Alzheimer’s disease: facts and fictions. *Frontiers in Molecular Neuroscience*, 4:17, 2011.
- J. Viinikka, A. Hyttinen, J. Pensar, and M. Koivisto. Towards scalable Bayesian learning of causal DAGs. *arXiv preprint arXiv:2010.00684*, 2020.
- L. Wasserman and K. Roeder. High dimensional variable selection. *Annals of Statistics*, 37(5A):2178, 2009.
- Y. Yuan, X. Shen, W. Pan, and Z. Wang. Constrained likelihood for reconstructing a directed acyclic gaussian graph. *Biometrika*, 106:109–125, 2019.
- Y. Zhang, M. J. Wainwright, and M. I. Jordan. Lower bounds on the performance of polynomial-time algorithms for sparse linear regression. In *Conference on Learning Theory*, pages 921–948, 2014.
- T. Zhao, H. Liu, T. Zhang, et al. Pathwise coordinate optimization for sparse learning: Algorithm and theory. *The Annals of Statistics*, 46(1):180–218, 2018.
- X. Zheng, B. Aragam, P. K. Ravikumar, and E. P. Xing. DAGs with NO TEARS: Continuous optimization for structure learning. In *Advances in Neural Information Processing Systems*, pages 9472–9483, 2018.